AD-A143 780 STABILITY OF LAMINAR ELECTRON LAYERS(U) NAVAL RESEARCH 1/1
LAB WASHINGTON DC D CHERNIN ET AL. 22 JUN 84
NRL-MR-5358 SBI-AD-E000 580

UNCLASSIFIED F/G 20/8 NL

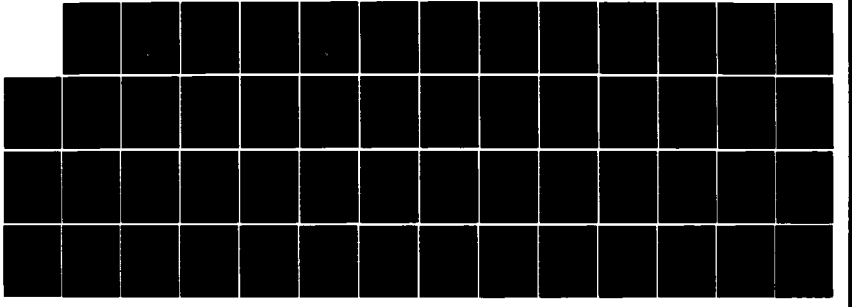

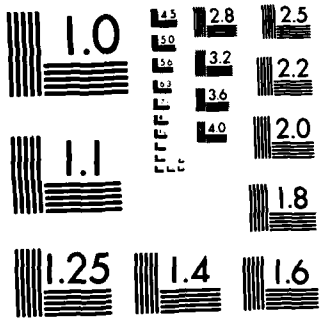

MICROCOPY RESOLUTION TEST CHART
NATIONAL BUREAU OF STANDARDS-1963-A

(2)

NRL Memorandum Report 5358

Stability of Laminar Electron Layers

D. CHERNIN* AND Y.Y. LAU

Plasma Theory Branch
Plasma Physics Division

**Science Applications, Inc.*
McLean, VA 22102

June 22, 1984

This work was supported by the Office of Naval Research.

NAVAL RESEARCH LABORATORY
Washington, D.C.

SECURITY CLASSIFICATION OF THIS PAGE

REPORT DOCUMENTATION PAGE

1a REPORT SECURITY CLASSIFICATION UNCLASSIFIED	1b RESTRICTIVE MARKINGS
2a SECURITY CLASSIFICATION AUTHORITY	3 DISTRIBUTION/AVAILABILITY OF REPORT Approved for public release; distribution unlimited.
2b DECLASSIFICATION DOWNGRADING SCHEDULE	
4 PERFORMING ORGANIZATION REPORT NUMBER(S) NRL Memorandum Report 5358	5. MONITORING ORGANIZATION REPORT NUMBER(S)
6a NAME OF PERFORMING ORGANIZATION Naval Research Laboratory 6b OFFICE SYMBOL (If applicable) Code 4790	7a. NAME OF MONITORING ORGANIZATION Office of Naval Research
6c ADDRESS (City, State and ZIP Code) Washington, DC 20375	7b. ADDRESS (City, State and ZIP Code) Arlington, VA 22217
8a NAME OF FUNDING/SPONSORING ORGANIZATION Office of Naval Research 8b OFFICE SYMBOL (If applicable)	9. PROCUREMENT INSTRUMENT IDENTIFICATION NUMBER
8c ADDRESS (City, State and ZIP Code) Arlington, VA 22217	10 SOURCE OF FUNDING NOS. PROGRAM ELEMENT NO: 61153N-11 / PROJECT NO: RR011-09-41 / TASK NO: / WORK UNIT NO: DN980-032
11 TITLE (Include Security Classification) Stability of Laminar Electron Layers	
12 PERSONAL AUTHOR(S) Chernin, D.* and Lau, Y.Y.	
13a TYPE OF REPORT Interim 13b TIME COVERED FROM 10/83 TO 9/84	14 DATE OF REPORT (Yr., Mo., Day) June 22, 1984 15 PAGE COUNT 54
16 SUPPLEMENTARY NOTATION This work was supported by the Office of Naval Research. *Science Applications, Inc., McLean, VA 22102	
17 COSATI CODES FIELD / GROUP / SUB GR	18 SUBJECT TERMS (Continue on reverse if necessary and identify by block number) Electron beams Microwave devices Plasma instabilities

19 ABSTRACT (Continue on reverse if necessary and identify by block number)

The stability of a finite thickness, laminar cylindrical shell of electrons rotating azimuthally and enclosed in a coaxial waveguide is considered. The equilibrium rotation of the electrons is supported either by a radial electric field, an axial magnetic field, or a combination of both. The stability problem is formulated exactly as an eigenvalue problem, including all relativistic and electromagnetic effects as well as all effects of self and applied equilibrium fields. An approximate dispersion relation, valid for thin beams, is obtained analytically and the classical results for the "longitudinal" modes, i.e., the negative mass, cyclotron maser, and diocotron instabilities and for the "transverse" mode are recovered in appropriate limits. The dispersion relation is relatively simple and is valid for arbitrary values of the equilibrium electric and magnetic fields and for arbitrary beam energy. It therefore provides a ready comparison of the small signal properties of such devices as the Astron, gyrotron, orbitron, heliotron and the various cross field devices. It may also be of interest in accelerator and space physics applications. Some heretofore unnoticed effects on beam stability

(Continues)

20 DISTRIBUTION AVAILABILITY OF ABSTRACT UNCLASSIFIED UNLIMITED X SAME AS RPT ☐ DTIC USERS ☐	21 ABSTRACT SECURITY CLASSIFICATION UNCLASSIFIED
22a NAME OF RESPONSIBLE INDIVIDUAL Y. Y. Lau	22b TELEPHONE NUMBER (Include Area Code) (202) 767-4148 22c OFFICE SYMBOL Code 4792

DD FORM 1473, 83 APR EDITION OF 1 JAN 73 IS OBSOLETE

SECURITY CLASSIFICATION OF THIS PAGE

19. ABSTRACT (Continued)

of equilibrium fields are reported; one such effect in particular leads to formulation of a simple, effective method either to maximize or eliminate altogether the longitudinal mode growth. Results from the dispersion relation compare favorably to results obtained from a numerical solution of the eigenvalue problem.

CONTENTS

STABILITY OF LAMINAR ELECTRON LAYERS

I. Introduction

There exists by now a truly enormous literature on the subjects of the equilibrium and stability of layers of charged particles in various geometries. The earliest studies[1-7] were conducted in order to understand the "slipping stream" or diocotron effect in the operation of the first magnetrons. Somewhat later the importance of curvature effects was realized when beams became relativistic, as in particle accelerators; the resulting "negative mass" instability[8,9] completely dominates the planar beam diocotron effect at sufficiently high energies (only a few tens of keV in many practical devices of interest). The negative mass effect was also investigated in connection with some controlled fusion research devices[10-12] and other machines.[13]

In recent times there has been renewed interest in high power, high efficiency microwave devices as well as in accelerators capable of high current operation. Spurred by the discovery of the electron cyclotron maser (or gyrotron) effect,[14-16] research in the field of short wavelength, high power microwave devices requiring no slow wave structure has been vigorously pursued.[17] Operation of these new devices depends fundamentally on the negative mass effect as enhanced by a synchronism of the particles' angular motion with the temporal and angular variation of a "cold" waveguide mode. This enhancement, though not called the maser effect, was first noted in the classic work of Briggs and Neil[10] and has been further elaborated in ref. 18.

The acceleration of large currents of electrons is a formidable problem which has also received considerable attention recently. In cyclic devices it is possible to construct high current equilibria in many cases[19-21] but various instabilities, the negative mass instability prominent among them, may limit achievable currents to smaller values than equilibrium considerations

Manuscript approved April 5, 1984.

alone would suggest. In these devices the effects of self fields on the negative mass instability and on the stabilization mechanism become important to consider; in one device these effects have been predicted to lead to a peculiar double-valued feature in the current vs. energy spread stability curve.[22] It was this particular result which initially prompted the study of self field effects reported here for a simpler (2D) model.

The model we consider consists of a layer of charged particles (we will think of them as electrons but ions may be trivially substituted) moving in circles about a common axis, as shown in Fig. 1. This restriction to laminar or "cold" electron flow will tend to overestimate actual growth rates of the modes we study since the effects of betatron oscillations and of nonaxis-encircling particles are stabilizing. An analysis including these effects is properly done in phase space using the correct equilibrium distribution function; such an analysis is significantly more complex than that given here and may be carried out only in an approximate way. The laminar flow case includes all essential physics and has great simplicity, allowing an exact treatment of the linearized problem, to recommend it. The equilibrium, discussed in the following section, is supported by a combination of self and externally applied radial electric and axial magnetic fields. We impose no a priori restriction on the relative magnitudes of the three terms--centrifugal force, electric force, $\vec{v} \times \vec{B}$ force--in the equilibrium force balance. This configuration is thus a reasonable model for the Astron,[23] magnetron, gyrotron, orbitron,[24] peniotron[25] and heliotron[26] and includes correctly the crucial radial and azimuthal particle dynamics found in particle accelerators. This "E-layer" model has the virtue that the linear stability problem may be formulated exactly, for arbitrary particle energies, including all effects of self fields and all effects of relativity and

electromagnetism. It is perhaps a bit surprising that, despite the venerability of the topic, this exact formulation has not been carried out earlier.[27] The eigenvalue problem governing the stability of the E-layer is derived and analyzed in Section III, below.

The desirability of a completely general treatment encompassing many devices and a large parameter space is related to the ease with which various familiar results for special cases may be recovered in appropriate limits. A dispersion relation for the so-called longitudinal mode obtained analytically in the thin beam limit from the ordinary differential equation governing the RF field reproduces all standard special case dispersion relations (negative mass, electron cyclotron maser, diocotron) in a straightforward way; in doing so, a puzzle is resolved concerning the survival of a finite negative mass growth rate in the planar limit and a method suggests itself on how either to maximize or eliminate altogether the negative mass instability growth.[28] Extensive testing of the dispersion relationship against a numerical solution of the eigenvalue problem shows excellent agreement, as reported in Section III. The classical diocotron dispersion relation is discussed and recovered from our formalism in Section IV.

Our treatment of the transverse mode, which has been invoked in the theory of the peniotron device[25] is somewhat less comprehensive. This mode is unstable only when electron motion is synchronous with a cavity mode and so is of a more specialized nature than the negative mass or diocotron instabilities which arise from intrinsic properties of geometry and shear flow, not from interaction with external structures. Still, the utility of the transverse mode for microwave generation may not yet have been fully exploited. We comment on some features of this mode in Section V.

II. Cold E-Layer Equilibrium

We consider an idealized model of an electron layer in which all electrons circle a common axis as shown in Fig. 1. We will neglect the effects of betatron oscillations and of axial motion in both perturbed and unperturbed states. Inclusion of betatron oscillations or axial perturbations is expected to have a stabilizing influence on the collective modes we will study. We further assume that in general the layer is enclosed in a coaxial waveguide with smooth, perfectly conducting walls at r=a and r=b, as shown in the figure. Absence of either or both walls results only in a change of certain boundary conditions.

Though this model is simple to describe it is surprisingly rich in content. Depending on beam and geometric parameters and types of applied fields, it may be taken as a good description of the Astron,[23] gyrotron,[17] orbitron,[24] peniotron,[25] heliotron[26] and cross field microwave devices and may also be of some interest in accelerator[8,9] and space physics stability problems as well as in the theory of magnetic insulation.

The equations governing the equilibrium quantities $v_o(r)\hat{\theta}$, $E_o(r)\hat{r}$, $B_o(r)\hat{z}$ for a specified density profile $n_o(r)$ are

$$\frac{\gamma_o v_o^2}{r} = \frac{e}{m}\left[E_o + v_o B_o\right] \tag{1}$$

$$\frac{1}{r}\frac{d}{dr}\left(rE_o\right) = -en_o/\varepsilon_o \tag{2}$$

$$\frac{dB_o}{dr} = \mu_o e n_o v_o, \tag{3}$$

where $-e$ and m are the electron charge and mass, γ_o is the usual relativistic factor, $\left(1-(v_o/c)^2\right)^{-1/2}$, c is the speed of light in vacuum, and ε_o and μ_o are

the permittivity and permeability of free space. In addition to the density profile, we take as given the total electrostatic potential difference and the total magnetic flux contained between r=a and r=b.

Using these conditions the solution to Eq. (2) is immediate and Eqs. (1) and (3) may be combined to yield a single differential equation for $u \equiv \beta_o\gamma_o \equiv v_o\gamma_o/c$:

$$u' = \frac{u}{r}\left[\frac{1 - \xi/\gamma_o^2 - \gamma_o^2 h}{1 + h}\right] \tag{4}$$

where $\xi = \omega_p^2/\omega_o^2$, $\omega_p^2 = e^2 n_o/m\gamma_o\varepsilon_o$ is the plasma frequency of the layer, $\omega_o = v_o/r$, and a prime denotes d/dr. In Eq. (4) we introduce the important quantity h, defined by,

$$h = \frac{erE_o}{mc^2\beta_o^2\gamma_o^3} \tag{5}$$

which is $(1/\gamma_o^2)$ times the ratio of the electric force to the centrifugal force experienced by an electron in equilibrium at radius r.

Equation (4) must be solved subject to an initial condition $u(r_1)$ satisfying Eq. (1) which we rewrite in the dimensionless form

$$u^2 = \alpha_E(u^2+1)^{1/2} + \alpha_B u \tag{6}$$

where $\alpha_E = erE_o/mc^2$ and $\alpha_B = erB_o/mc$. α_E is known at r_1 but α_B is not. The entire equilibrium problem then reduces to choosing $\alpha_B(r_1)$ such that the resulting total flux

$$\Phi_o = 2\pi\int_a^b dr\ rB_o \tag{7}$$

is a specified number. A numerical method for doing this is described in Appendix A. Here we briefly consider the character of some of the solutions. The equilibrium thus constructed will be used in the numerical solution of the eigenvalue problem in Section III.

Given $\alpha_E(r_1)$ and $\alpha_B(r_1)$, Eq. (6) may have 0, 1, or 2 real valued solutions for $u(r_1)$, depending on the values of α_E and α_B; without loss of generality we take $\alpha_B(r_1) > 0$. The situation in the α_E- α_B plane is then depicted in Fig. 2. By a positive root, denoted by (+) in the figure, we mean a right-handed rotation about $\vec{B}$ (clockwise, looking in the direction of $\vec{B}$). The equation for the boundary curve C in Fig. 2 is the condition for Eq. (6) to have a double root:

$$\alpha_E = \frac{u^*(u^*-\alpha_B)}{(u^{*2}+1)^{1/2}} \tag{8}$$

where $u^* = (8/3)^{1/2}\sinh\left[\frac{1}{3}\sinh^{-1}\left[\frac{1}{2}(3/2)^{3/2}\alpha_B\right]\right]$. On C, $1 + h = 0$.

There are three basic types of equilibria found in devices of practical interest: Type I, in which a magnetic field is used to balance centrifugal force (α_E is small, e.g. Astron, gyrotron, particle accelerators); Type II, in which electric and magnetic forces balance (inertia is small, e.g. crossed field microwave devices); and Type III, in which an electric field is used to balance centrifugal force (α_B is small, e.g. orbitron, heliotron). Type I may have only "+" roots while Types II and III may have either "+" or "-" roots. In the following analysis, however, we make no assumption regarding the relative magnitudes of the electric field, magnetic field, and inertia terms.

It is reasonable to ask whether stability considerations favor one type of equilibrium over another for a layer of given kinetic energy. To our knowledge there has been no definitive answer to this fundamental question.

For radiation source applications one arguably might want the most unstable configuration while for other applications, like accelerators, one would want the most stable one. We proceed to examine the stability of a general equilibrium describable by Eqs. (1) - (3) in order to address this question, our goal being a complete parametric study of the small signal behavior.

III. Stability of the Layer

We consider perturbations on the equilibrium described in the previous section. The equations governing the layer are, simply

$$(\frac{\partial}{\partial t} + \vec{v}\cdot\vec{\nabla})\gamma\vec{v} = -\frac{e}{m}(\vec{E} + \vec{v}\times\vec{B}) \qquad (9)$$

$$\vec{\nabla}\times\vec{E} = -\frac{\partial\vec{B}}{\partial t} \qquad \vec{\nabla}\cdot\vec{E} = -en/\varepsilon_o \qquad (10a,b)$$

$$\vec{\nabla}\times\vec{B} = \frac{1}{c^2}\frac{\partial\vec{E}}{\partial t} - \mu_o en\vec{v} \qquad \vec{\nabla}\cdot\vec{B} = 0 \qquad (11a,b)$$

where n is the number density.

Our discussion will be limited to consideration of perturbations in the $\hat{r}$ and $\hat{\theta}$ directions, for reasons described below. Writing all quantities Ψ as

$$\Psi(r,\Theta,t) = \Psi_o(r) + \sum_{\ell}\int\frac{d\omega}{2\pi}\, e^{-i(\omega t-\ell\Theta)}\Psi_1^{(\ell)}(r;\omega) \qquad (12)$$

where $\Psi_o(r)$ is the equilibrium value, and retaining only terms linear in $\Psi_1^{(\ell)}$ one finds that the linearized versions of Eqs. (9) - (11) decouple into two sets governing $\{v_{1r},v_{1\Theta},E_{1r},E_{1\Theta},B_{1z},n_1\}$ and $\{v_{1z},E_{1z},B_{1r},B_{1\Theta}\}$ which we identify as TE modes and TM modes respectively. (Here and below we

write $\Psi_1^{(\ell)}(r;\omega)$ simply as Ψ_1 for all first order quantities.) The TM modes may easily be shown to be neutrally stable for perfect conductor boundary conditions (damped for resistive wall boundary conditions). They represent simple oscillations of the electrons along the $\hat{z}$ direction in response to the cavity mode fields; the equilibrium model does not provide any free energy to excite the TM modes. The TE modes, on the other hand, are potentially unstable. If we had allowed a finite axial wavelength for the perturbed quantities the TM and TE modes would be coupled, but it has been found[10] that the effects of finite axial wavelength are stabilizing for the coupled case. Consequently we focus attention exclusively on the TE waves.

The Euler equation (9), upon linearization, gives the fluid response in terms of the RF fields of the TE wave:

$$-i\Omega v_{1r} - \omega_o P v_{1\theta} = -\frac{e}{m\gamma_o}[E_{1r} + v_o B_{1z}] \tag{13a}$$

$$\omega_o Q v_{1r} - i\Omega v_{1\theta} = -\frac{e}{m\gamma_o^3} E_{1\theta} \tag{13b}$$

where we have defined $\Omega = \omega - \ell\omega_o$, $P = \gamma_o^2(1+h)$, $Q = v_o'/\omega_o + h$, and $v_o' \equiv \frac{d}{dr} v_o$. Using the solution of Eqs. (13a,b) in the definitions of the RF currents J_{1r} and $J_{1\theta}$ and combining the linearized Maxwell's equations (10) - (11) allows one to write a single differential equation for $\phi \equiv rE_{1\theta}$:

$$r\frac{d}{dr}\left(r\tilde{A}\frac{d\phi}{dr}\right) + \tilde{C}\phi = 0 \tag{14}$$

where

$$\tilde{A} = \Delta^{-1}[1 + \xi/(D\gamma_o^2)] \tag{15}$$

$$\tilde{C} = \frac{\omega}{\Omega}\Big[\Big(\frac{\Omega}{\omega} - \frac{1}{\gamma_o^2}\Big)\frac{r}{\omega_o}\frac{\partial}{\partial r}\big(\omega_o\Delta^{-1}D^{-1}\xi(1+h)\big) + 2\beta_o^2\Delta^{-1}D^{-1}\xi(1+h)\Big]$$

$$+\Delta^{-1}D^{-1}(\xi/\gamma_o^2)\Big(\frac{\omega^2r^2}{c^2} - \ell^2 - \xi\beta_o^2\Big) + 1 \tag{16}$$

$$\Delta = \frac{\omega^2r^2}{c^2} - \ell^2 + D^{-1}\xi(\Omega^2r^2/c^2) \tag{17}$$

$$D = PQ - \Omega^2/\omega_o^2 = 1 - \xi/\gamma_o^2 + \gamma_o^2h^2 - \Omega^2/\omega_o^2 \tag{18}$$

and other symbols have been defined previously. [Equation (14) is identical to Eq. (4) of Ref. 28, except for a few differences in notation.]

The other RF fields are given in terms of ϕ by

$$E_{1r} = ir\Delta^{-1}\Big[\Big(\frac{\ell}{r} + \xi D^{-1}\Omega v_o/c^2\Big)\phi' - \frac{\omega\omega_o}{c^2}\xi D^{-1}(1+h)\phi\Big] \tag{19}$$

$$B_{1z} = -\frac{ir}{c^2}\Delta^{-1}\Big[(\omega + \xi D^{-1}\Omega)\phi' - \frac{\ell}{r}\omega_o\xi D^{-1}(1+h)\phi\Big] \tag{20}$$

and the perturbed velocities may be easily recovered using Eqs. (19) and (20) in Eqs. (13a,b); the perturbed density is obtained from $n_1 = -(\varepsilon_o/e)\vec{\nabla}\cdot\vec{E}_1$.

Equation (14) must be solved subject to $\phi(a) = \phi(b) = 0$ (if the walls are perfect conductors) in order to obtain the eigenvalue, ω. Hereafter we shall assume that the electron layer is restricted to the annular region $r_1<r<r_2$ [Fig. 1]. In this case it is convenient to formulate the problem using the explicit vacuum solutions at $r=r_1$ and $r=r_2$ and to match the appropriate logarithmic derivatives, as is often done in microwave tube theory, in order to isolate the effect of wall boundary conditions. Defining, then, the

normalized admittances evaluated just outside of the layer, we have

$$b_+ \equiv -\left.\frac{iE_{1r}}{E_{1\theta}}\right|_{r=r_2^+} = \left.\frac{\ell r_2}{\frac{\omega^2 r_2^2}{c^2} - \ell^2}\,\frac{\phi'}{\phi}\right|_{r=r_2^+} \tag{21a}$$

$$b_- \equiv \left.\frac{iE_{1r}}{E_{1\theta}}\right|_{r=r_1^-} = \left.\frac{-\ell r_1}{\frac{\omega^2 r_1^2}{c^2} - \ell^2}\,\frac{\phi'}{\phi}\right|_{r=r_1^-} . \tag{21b}$$

We stress that the normalized wave admittances b_+ and b_- depend only on the waveguide geometry exterior to the electron beam. They are independent of the beam or its dynamics. b_+ and b_- are evaluated explicitly in Appendix B for some practical cases of interest.

Let us examine Eq. (14) more closely. In the complex r plane Eq. (14) has singularities at points where

$$\omega - \ell\omega_o = 0 \tag{22}$$

$$D + \xi/\gamma_o^2 = 0 \tag{23}$$

$$\Delta = 0. \tag{24}$$

The first of these clearly represents a match between the mode frequency and a harmonic of the particle "cyclotron" frequency. Such a match is present in the negative mass instability, cyclotron maser instability, and diocotron instability all of which are described by Eq. (14). Indeed, these may all be considered to be the same instability in this sense,[18] though the individual names are still useful. The negative mass instability is fundamentally a rotational effect. The classical explanation attributes it to the decrease of circulation frequency with particle energy leading to growth of azimuthal bunches. The negative mass instability operates without regard for the cavity

modes of the vacuum chamber; the fields are not well approximated by the cavity mode. The instability is strongly enhanced however if Re(ω) happens to be a cavity mode, as first pointed out by Briggs and Neil.[10] In recent years this synchronous case has been given its own name, the cyclotron maser instability, mainly in the literature of gyrotron research.[17,18]

The diocotron instability, originally studied in connection with the development of the first cross field microwave devices, is a "residual" instability in this context. It is what survives in the non-relativistic and/or planar limits. The perturbed electric fields are basically electrostatic in nature and are strongly localized at the position of the layer. The equation governing the diocotron instability[1,4,6,7,29] may be recovered formally from Eq. (14) by taking $c \to \infty$. It is discussed further in Section IV, below.

A mode satisfying Eq. (22) is sometimes called the longitudinal mode since the major effect on the beam is azimuthal bunching. Equation (23), on the other hand, describes what has been called the transverse mode which involves little bunching, but significant transverse (radial) motion of the beam. If h is small, Eq. (23) becomes

$$\omega - \ell\omega_o = \pm\, \omega_o . \qquad (25)$$

This transverse mode has been invoked to explain the operation of the peniotron[25] when ω corresponds to a cavity mode. In the nonsynchronous case the transverse mode is stable in the absence of resistive walls, as pointed out in ref. 10.

Finally we note that Eq. (24) may be loosely associated with an electromagnetic mode. In vacuum only (24) survives as a singularity but in

fact it may be shown to be only an "apparent" singularity;[30] the vacuum eigenfunctions are analytic in r, except possibly at r=0.

We proceed to analyze Eq. (14) to uncover the parametric dependences of the growth rates of the unstable modes. In order to make progress analytically we consider the case of a beam of uniform density and of thickness $\tau \equiv r_2 - r_1$ which is much less than its average radius $R \equiv \frac{1}{2}(r_2 + r_1)$. If the beam is sufficiently thin it is possible to consider a Taylor series solution about r=R of Eq. (14), taking care to check at the end that the singularities are sufficiently far away in the complex r plane, so as not to disturb the series convergence;[31] carrying out this program we find the dispersion relation

$$G_+ - G_- + \tau\left[\frac{C_o}{R^2 A_o} + \frac{1}{2}(G_+ + G_-)\left(\frac{A_1}{A_o} + \frac{1}{R}\right) + G_+ G_-\right]$$

$$- \frac{3}{8}\left(\frac{\tau}{R}\right)^2 (G_+ - G_-)\left(\frac{C_o}{A_o}\right) = 0 \qquad (26)$$

correct to order $(\tau/R)^2$. In Eq. (26) G_-, G_+ are the radial logarithmic derivatives of ϕ evaluated just <u>inside</u> the layer at $r=r_1$, $r=r_2$ respectively, obtained by integrating Eq. (14) across the beam edges:

$$G_\pm = \frac{-1}{r_{2,1}\tilde{A}(r_{2,1})}\left[\mp \frac{1}{\ell} b_\pm + q(r_{2,1})\right] \qquad (27)$$

where

$$q(r) = \frac{\omega}{\Omega}\left(\frac{\Omega}{\omega} - \frac{1}{\gamma_o^2}\right)\frac{\xi(1+h)}{\Delta D} \qquad (28)$$

and

$$\tilde{A}(r) \simeq A_o + (r-R)A_1 + \cdots \qquad (29)$$

$$\tilde{C}(r) \simeq C_o + \cdots$$

near r=R.

Expanding $G_\pm$ to order τ/R, Eq. (26) then reduces to

$$\frac{1}{\ell}(b_+ + b_-) + \frac{\tau}{R}\left[-Rq' - \frac{1}{A_o}(\frac{1}{\ell}b_+ - q)(\frac{1}{\ell}b_- + q) + C_o\right] = 0 \qquad (30)$$

where now q and q′ are understood to be evaluated at r=R and where in Eq. (30) we have (temporarily) kept terms only to $O(\tau/R)$. No assumption has been made about the E-layer density or current; we have assumed only that the beam is "thin".

Let us first consider the longitudinal mode, that is, we look for a root of Eq. (30) with $|\Omega^2| << \omega_o^2$. Of the terms within the brackets in Eq. (30) only the q' and q^2 terms behave as Ω^{-2} for small Ω. Keeping only such terms, some algebra gives $\Omega_1 \equiv \mathrm{Im}(\Omega)$:

$$\Omega_1^2 \equiv \frac{\ell \frac{\tau}{R}\omega_p^2}{(b_+ + b_-)} \frac{(\beta_o^2 + 2h)}{(1 + \gamma_o^2 h^2)} + O(\ell\tau/R)^2 \qquad (31)$$

which, for h = 0, is the classical negative mass dispersion relation for the Astron configuration.[10] (The $O(\ell\tau/R)^2$ term is displayed fully in Eq. (36), below.) We remark that Eq. (31), including the second order terms, can be obtained from the much simplified form of Eq. (26),

$$G_+ - G_- + \tau G_+ G_- = 0 \qquad (26')$$

where terms behaving as Ω^{-1} have been dropped from Eq. (26).

Ignoring the $O(\ell\tau/R)^2$ term in Eq. (31) for a moment, we may interpret the dispersion relationship (31) as follows. As we have seen, the factor $(b_+ + b_-)$ represents the effects of the container structure, and the factor $(\tau/R)\omega_p^2$ is proportional to the beam current. These two terms always appear in any dispersion relation involving an electron beam. All dynamical effects, including those due to self fields, are contained in the factor

$$M \equiv - \frac{(\beta_o^2 + 2h)}{(1 + \gamma_o^2 h^2)} \tag{32}$$

for a sufficiently thin beam. Some insight into the meaning of this factor may be had if we note that for small equilibrium densities, ξ, it is proportional to $d\omega_o/d\varepsilon$ where $\varepsilon = mc^2\gamma_o - e\phi_o$ is the total energy of a particle in the equilibrium:

$$\gamma_o \beta_o^2 \frac{d\omega_o}{d\varepsilon} = \frac{-\omega_o}{mc^2}\left[\frac{\beta_o^2 + 2h + \xi/\gamma_o^4}{1 + \gamma_o^2 h^2 - \xi/\gamma_o^2}\right]. \tag{33}$$

At least when ξ is small then we find agreement with the classical explanation of the negative mass effect: A rotating beam is unstable (stable) if its equilibrium rotation frequency is a decreasing (increasing) function of its (total) energy, that is, M is proportional to the effective azimuthal inertia (mass). We stress that for finite ξ this interpretation begins to break down; Eq. (31) was derived assuming ξ was finite yet ξ does <u>not</u> appear in the factor M but clearly does appear in Eq. (33).

M, though simple in form, has many interesting features. Let us consider its dependence on h, illustrated in Fig. 3. Perhaps the most interesting property of M is that it experiences a change in sign at $h = -\beta_o^2/2$. The possibility for using this property of equilibria supported by a radially

inward electric field in addition to a magnetic field in order to suppress the negative mass instability has been discussed elsewhere.[28] We note that since the factor M is independent of the beam current or of the waveguide dimensions and represents a purely dynamical quantity, this stabilization of the negative mass instability by a radial electric field is expected to be valid even in toroidal geometry, even for high current, very cold beams. (The method is limited to use for moderately low energy beams, in the MeV range in practice, since the applied electric field required to change the sign of M from negative to positive is proportional to γ_o^3, as follows from the definition of h, Eq. (5).) Note that there is a "most stable" configuration at h=-1, at which point certain singular parts of $\tilde{C}$ in Eq. (14) vanish identically.

Perhaps equally interesting for microwave generation applications, is the occurrence of a "most unstable" point in Fig. 3 at $h = 1/\gamma_o^2$. If we recall that $\gamma_o^2 h$ is the ratio of the radial electric force to the centrifugal force we observe that the choice $\gamma_o^2 h = 1$ describes a configuration in which the equilibrium is supported solely by an electric field (a Type III equilibrium, in the language of Section II). This result suggests that for a given beam energy, a microwave source such as the orbitron[24] in which an annular beam circles a positively charged wire with no applied magnetic field, might have some advantage over more conventional devices like magnetrons (h<0), inverted magnetrons ($h>>1/\gamma_o^2$), or gyrotrons($h\approx 0$). This finding is novel. We remark that this negative peak in M is sharpest at low energies (small β_o^2).

In the non-relativistic limit, $\beta_o^2 \to 0$, $\gamma_o^2 \to 1$, the sign of M is determined directly by the sign of h, which remains finite in this limit. Usually we are accustomed to thinking that the negative mass instability should vanish in the non-relativistic limit when there is no gradient in the magnetic field. Here we see however that an equilibrium electric field can affect the sign of

the azimuthal inertia just as a gradient in B can. If we define an equivalent field index, n_{eq}, by

$$\frac{1}{1-n_{eq}} - \frac{1}{\gamma_o^2} \equiv -M \tag{34}$$

then

$$n_{eq} = h\left[\frac{2 - (\gamma_o^2-1)h}{(1+h)^2}\right] \tag{35}$$

which vanishes when h does.

One final comment about h must be made. The electric field appearing in the definition of h, Eq. (5), is due both to the electric charge of the layer and to any externally applied bias potential. When the contribution of the electric charge dominates there is some question as to what value of h to use in Eq. (31) when calculating growth rates since E_o and therefore h will change sign somewhere within the layer. For this reason, in all numerical examples considered below we will assume that h, when it is non-negligible, is dominated by the contribution of an externally maintained bias potential.

The analytical results presented up to this point are subject to test by numerical integration of Eq. (14) subject to suitable boundary conditions. We have written a program to carry out this task. Given a density profile, the electrostatic potential difference and the total magnetic flux contained between r=a and b, the program calculates all equilibrium quantities then, given the mode number ℓ, locates an eigenvalue ω. In all examples below the density profile is parabolic; we expect good agreement with Eq. (31), derived using a flat profile, if we identify $(\tau/R)\,\omega_p^2$ with $2(\nu/\gamma_o)(c^2/R^2)$ where ν is Budker's parameter, the number of particles per unit length times the

classical electron radius. All examples use a perfectly conducting wall; effects of a small wall resistivity, which may be very important under some conditions, are discussed briefly toward the end of Appendix B.

Though we shall eventually test Eq. (31) for all parameter dependences, let us first check the interesting dependence on h, discussed above, against a numerical solution of Eq. (14). Figure 4 presents some typical results. Here we have illustrated, for two different values of ν/γ_o a comparison of the $\ell = 1$ mode growth rates for a thin ($\tau/R = .02$) beam as predicted by Eq. (31) (dashed line) and by a solution of Eq. (14) (solid line). (To be precise, what is plotted on the numerical solution curve is $\mathrm{Im}(\omega)/\omega_o(r_1)$.) The transition from stable to unstable behavior occurs at $h = -\beta_o^2/2$ ($\simeq -0.278$ for this case) <u>independent</u> of ξ. This is an important feature of Eqs. (31) and (32) which has been used to argue[28] that the stabilization condition, $h<-\beta_o^2/2$, for the negative mass instability is independent of the beam current. Note that this statement cannot be made on the basis of single particle orbit theory alone [cf. Eq. (33)]; the stabilization condition is obtained from collective mode considerations including self field effects. Actually a small amount of residual growth remains for h less than but very close to $-\beta_o^2/2$, a feature discussed in more detail in the following section. Agreement between Eq. (31) and the numerical solution is best at small growth rates which is reasonable if we recall that terms behaving as Ω^{-1} were neglected in favor of terms behaving as Ω^{-2} when Eq. (31) was derived. Equation (31) consistently gives slightly too high a growth rate (i.e. it is pessimistic), a feature which will be shown to persist when variations of other parameters are considered. Notice that the numerical solution confirms the existence of a peak in the growth rate for $h = 1/\gamma_o^2$, as predicted by Eq. (31), again independent of ξ.

The significant parameters upon which the small signal behavior of the layer depends include, beside the externally applied bias fields, the geometry factors a, b, r_1, r_2, the current (ν), the beam energy γ_o, and the mode number ℓ. We proceed to consider the effect of each of these separately on the growth rate of the longitudinal mode, $\omega \approx \ell\omega_o$, for the specific case of an Astron-like configuration, $h \approx 0$.

Unless otherwise stated all parameters in the cases considered below will take the following nominal "base case" values: $a = 0.5$m, $b = 2.2$m, $r_1 = 0.99$m, $r_2 = 1.01$m, total electrostatic potential difference between inner and outer walls = 0., total flux between inner and outer walls = $\pi(b^2 - a^2)\, B_{oo}$ where $B_{oo} = 48.2\times10^{-4}$T is the field required to hold a single particle at R = 1m with $\gamma = 3$. The radial density profile is always taken to be parabolic and symmetric about r=R=1m with specified peak value; the base case value is 5×10^7/cc which gives $\nu/\gamma_o = 3.94\times10^{-3}$. The base case azimuthal mode number ℓ is 1, for which $b_+ + b_- \tilde{=} 2.50$ for $\omega = \omega_o$. From Eq. (31) the normalized growth rate for the base case is 5.6%; the numerical solution of the eigenvalue problem gives 5.35%.

Figure 5 illustrates the comparison of growth rates as calculated by Eq. (31) and by a numerical solution of the eigenvalue problem for a range of currents. Over the wide range considered, the $\nu^{1/2}$ scaling predicted by Eq. (31) is shown to hold up extremely well up to values of ν/γ_o of a few percent. Similar excellent agreement is generally found for variations in layer thickness (Fig. 6), outer wall position (Fig. 7), inner wall position (Fig. 8), particle energy (Fig. 9), and azimuthal mode number (Fig. 10). Some remarks on each case follow.

In the case of varying layer thickness with the maximum density fixed (Fig. 6) two effects are competing; these are the basic $\nu^{1/2}$ dependence of the

growth rate versus the stabilizing effect of finite thickness[30] (effectively, finite frequency spread). The finite thickness effect is clearly second order in (τ/R) and is not shown explicitly in Eq. (31) but it is included in all plotted data of Figs. 5 - 10; the second order term is given explicitly in the following section. In the examples we have studied, finite thickness effects have been small and have not been effective in stabilizing the instability.

In Fig. 7 the effect of outer wall position is illustrated. As the wall is moved in from its base case location at 2.2m the growth rate is observed to increase dramatically for a while, then to fall off. The reason for the increase is the approach to synchronism of particle motion with a cavity vacuum mode, that is, $\omega \approx \ell\omega_o \approx \omega_v$ where ω_v is a solution to $b_+ + b_- = 0$; under this synchronous condition the cavity mode fields act to enhance those established by the dynamical charge bunching due to the negative mass effect. This synchronous case has been given its own name, the cyclotron maser instability, and is put to enormous practical use in the gyrotron family of microwave devices.[17] While in Figs. 5 - 10 we have consistently evaluated b_+ and b_- at $\omega = \ell\omega_o$, near a zero of $b_+ + b_-$ this is clearly inadequate and Eq. (31) should be solved as a cubic polynomial. Empirically we find that evaluating $b_+ + b_-$ at $\omega = \ell\omega_o$ is adequate when $b_+ + b_- > \ell$.

As the outer wall is moved further inward, past the synchronous point the growth rate in Fig. 7 drops as $b_+ + b_-$ changes sign. This drop is attributable to a "shorting out" of the azimuthal field $E_{1\theta}$ as the wall approaches the edge of the layer. An identical phenomenon is seen as the inner wall is moved outward, Fig. 8. Use of an inductive impedance ($b_+ + b_- < 0$) to stabilize the negative mass instability has been proposed by Briggs and Neil.[32] We remark that in Fig. 8 no synchronous case is encountered for the parameters considered, as the inner wall is moved.

The decrease of growth rate with increasing kinetic energy is documented in Fig. 9. The basic reason for this decrease is just the relativistic mass increase: the azimuthal response of a particle to the perturbed field $E_{1\theta}$ is reduced by a factor γ_o^{-1}, for large γ_o. No synchronous cases are encountered over the range of γ_o considered.

In Fig. 10 we have plotted growth rate versus azimuthal mode number ℓ. Agreement is good between the dispersion relation, Eq. (31), and the numerical solution; near synchronous cases occur for $\ell = 5$ and 9. Though predicted growth rates are rather large, for the high ℓ modes, these should in practice be subject to stabilization by the effects of finite betatron oscillations which we have neglected in this treatment. In any event we expect the dispersion relation, Eq. (31), to begin to break down for short wavelengths, i.e. $\ell\tau/R \gtrsim O(1)$, or azimuthal wavelengths on the order of the layer thickness. A WKB treatment of Eq. (14) carried out for this case yields an eigenvalue condition, the numerical solution to which would appear to require more effort than a direct numerical solution of Eq. (14) itself.

Finally, we report that in the initial phase of our investigation, we attempted to derive the dispersion relationship by constructing a quadratic form for the differential equation (14), under the assumption that $\phi = rE_{1\theta}$ is approximately continuous across the E-layer. The latter assumption has been widely used and has been considered valid[9-11,17,18] for a thin relativistic electron beam. However, this line of investigation led to an incorrect dispersion relationship if $\omega_p^2/\omega_o^2 \gtrsim O(1)$, even to the lowest order in τ/R. In other words, to account correctly for the DC self fields in the present Eulerian description, the tangential AC electric field should not be assumed constant across the E-layer, regardless of the thickness. On the other hand, our dispersion relationship Eq. (31) correctly accounts for the self fields,

and is valid for arbitrary beam energy, and arbitrary combination of E_o and B_o, as already stressed.

IV. Residual Growth: The Diocotron Instability

Sufficiently close to the "zero mass" points $h \approx -\beta_o^2/2$, $h \to \pm\infty$, Eq. (31) begins to be dominated by the neglected terms of order $(\tau/R)^2$. We have already observed this phenomenon near the point $h = -\beta_o^2/2$ in Fig 4. In this section we discuss the point $h \to \pm\infty$, which extreme is reached in the planar limit: $r \to \infty$, $\ell \to \infty$, $\ell/r \equiv k_y$ finite. We remark that the vanishing of the negative mass growth rate in the planar limit, a feature of Eq. (31) and clearly expected on physical grounds, has not previously been demonstrated analytically, to the authors' knowledge.

The second order term in Eq. (31) is given, in complete generality, by $(\ell\tau/R)^2\omega_o^2\Lambda$ where

$$\Lambda = \frac{1}{4\gamma_o^6(1+h)^2(1+\gamma_o^2h^2)}\left[\xi^2(\beta_o^2 + 2h + (1+h)^2)\right.$$

$$\left.+2\xi\gamma_o^4\,(\beta_o^2 + 2h)^2 - \gamma_o^6(1+\gamma_o^2h^2)(\beta_o^2 + 2h)^2\right]$$

$$-\left[\frac{\xi}{2}\,\frac{(1+h)}{\gamma_o^2(1+\gamma_o^2h^2)}\,\left(\frac{b_+ - b_-}{b_+ + b_-}\right)\right]^2. \qquad (36)$$

As it stands Λ includes both the diocotron instability (ξ^2 terms) and the finite thickness stabilization effect[30] (ξ^o term) referred to above. The last term of Eq. (36) contains wall boundary effects; specifically we may recover the stabilization at the diocotron mode due to contact of the layer with perfectly conducting walls,[6] as well as the destabilizing effects of finite wall conductivity.[34-37] If we assume that the walls are many wavelengths away

and that the fields are electrostatic then, in the planar limit, $b_{\pm} = 1$. Taking, then, the planar limit, $h\omega_o \to -eB_o/(m\gamma_o^3) \equiv -\omega_c/\gamma_o^2$, only the first ξ^2 term in Eq. (36) survives and we recover the classical result[4] for the growth rate of the diocotron mode

$$\mathrm{Im}(\omega) \approx |k_y \tau v_o'/2| \tag{37}$$

where the velocity shear $v_o' = \omega_p^2/(\omega_c \gamma_o^2)$. Of course Eq. (37) may be obtained by much simpler methods than those employed here; our point is only that it is recoverable from the present formalism. Note that the dependence on the line density, ν, of the diocotron growth rate is just ν^1; for the (non-synchronous) negative mass instability the dependence is $\nu^{1/2}$; for the synchronous case it is $\nu^{1/3}$.

The relationship between the diocotron and negative mass instabilities has been discussed by Neil and Heckrotte[38] and by Lau.[18] Mostrom and Jones[39] have recently examined the electrostatic case, including the effects of shear in v_z. Davidson and Tsang[29] have reported analytical and numerical results in cylindrical geometry.

V. The Transverse Mode

An electron moving in a field satisfying Eq. (25) where $\mathrm{Re}(\omega)$ is a vacuum guide mode may be shown to be acted upon by a nearly constant electric field, when the motion is averaged over its gyro-orbit. The particle therefore experiences an $\vec{E} \times \vec{B}$ drift transversely, toward the wall, which motion brings the particle to experience yet a stronger electric field. A net transfer of energy from (to) the particles may be shown to result for the - (+) sign resonance of Eq. (25). This mechanism of wave growth has been used to explain

the operation of the peniotron oscillator.[25]

In the planar limit of the previous section, the resonance condition for the transverse mode, Eq. (23), becomes $\gamma_o(\omega - k_y v_o) = \pm \omega_c$, which is the well-studied mode of planar magnetron tube theory.[1-7,33,34] The factor h, [Eq. (5)], thus again appears, as it did in Eq. (31), as a measure of the "planarity" of the configuration.

A dispersion relation for the transverse mode may also be obtained from Eq. (30). Keeping the most important terms we have, approximately

$$\frac{1}{\ell}(b_+ + b_-) - \frac{\tau}{R}\frac{1}{A_o}\left(\frac{1}{\ell}b_+ - q\right)\left(\frac{1}{\ell}b_- + q\right) = 0 \qquad (38)$$

where, near the zeroes of A_o

$$A_o \simeq \frac{-(\Omega^2 - \alpha^2\omega_o^2)}{\ell^2\omega_p^2\left(1 - \beta_o^2\frac{\omega}{\ell\omega_o}\right)^2} \qquad (39)$$

$$q \simeq \frac{-\omega_o}{\ell\Omega}\,\frac{(1+h)}{\left(1 - \beta_o^2\frac{\omega}{\ell\omega_o}\right)} \qquad (40)$$

where $\alpha^2 = 1 + \gamma_o^2 h^2$. Equation (38), using Eqs. (39) and (40), agrees with Eq. (39) of Briggs and Neil[10] for h = 0, to leading order in ξ.

Clearly there are no unstable roots of Eq. (38) near the (simple) zeroes of A_o unless either one of these nearly coincides with a zero of $b_+ + b_-$ (a guide mode cutoff frequency) or b_+ or b_- contains an imaginary part, due to finite wall resistivity for example (see Appendix B). Thus the transverse mode (for small h) depends crucially on the interaction of the electrons with their external surroundings, unlike the negative mass and diocotron instabilities, the mechanisms of which operate in a manner that is insensitive to boundary conditions on the fields at distant walls. In the synchronous

case, with perfectly conducting walls the predicted scaling of the growth rate of the transverse mode with ν is $\nu^{1/2}$. The dependence of the real part of the frequency of the mode on an externally applied radial DC electric field may prove useful in some circumstances.

The peniotron interaction is essentially non-relativistic. It relies heavily on the spatial inhomogeneity of the perturbed wave fields. In contrast, for longitudinal modes, the spatial inhomogeneity of the unperturbed motion (i.e. shear) is far more important. Both the transverse and longitudinal modes can be used to convert the rotational energy of the electrons to rf waves efficiently, however.

In the planar limit Eq. (38) continues to predict stability in the absence of a resistive wall yet it is well-known[1-5] that inclusion of a resonant layer satisfying $\gamma_o(\omega - k_y v_o) = \pm \omega_c$ in the beam leads to wave growth. The resolution of this contradiction lies in the failure of the Taylor series solution to Eq. (14), from which Eq. (38) was obtained; the resulting growth rate is non-analytic in ξ and one must resort to numerical or other methods[7] to solve the eigenvalue problem.

VI. Summary

In this paper we have attempted a general treatment of the linear stability problem for laminar electron flow in cylindrical geometry. The basic equilibrium state has been taken to be maintained by radial electric and/or axial magnetic fields (Eq. (1)). No azimuthal magnetic field nor any axial electron motion have been included in the equilibrium state. The linear stability problem for azimuthal and radial perturbations has been formulated exactly, fully relativistically and fully electromagnetically, including all effects of self fields. The stability problem reduces to an eigenvalue problem for the frequency ω, given the azimuthal mode number, ℓ (Eq. (14), with associated boundary conditions).

Our efforts have been focused on the longitudinal mode (Eq. (22)), for thin beams, which is of considerable importance in accelerator and microwave device research. We have obtained, and favorably compared to a numerical solution of the eigenvalue problem, a dispersion relation in the thin beam limit (Eq. (31)) which applies in complete generality to the longitudinal mode and which reproduces all classical results in appropriate limits. Some interesting differences among equilibria regarding the negative mass instability have been pointed out; namely we have found a simple way either to stabilize or to maximize the growth of this mode. This finding might have practical consequences in accelerator or microwave tube design.

The longitudinal mode, $\omega - \ell\omega_o \approx 0$, encompasses the negative mass, electron cyclotron maser, and diocotron instabilities. The negative mass and electron cyclotron maser effects are unique to cylindrical geometry; they are fundamentally relativistic in nature when the motion is supported solely by a magnetic field. They are even more pronounced, especially for low energy beams, if the equilibrium rotation is supported solely by a radial electric

field. In planar geometry both of these instabilities are absent and only the residual diocotron instability remains which itself may be stabilized by placing the layer in contact with a conducting wall.[6]

The transverse mode, $\omega - \ell\omega_o = \pm \alpha\omega_o$ (α is defined following Eq. (40)) has been used to explain the operation of the peniotron device. When the geometry is cylindrical ($|\gamma_o h| \ll 1$) this mode is stable unless the electron motion is synchronous with a cavity mode and/or resistive walls are present. In the planar limit $\alpha\omega_o \to \omega_c/\gamma_o$ and we identify this mode as the Doppler shifted cyclotron resonance considered by Buneman[4,5] and others[1,6,7,33] in studies of magnetron operation. This mode is the dominant unstable mode for planar, high density laminar flow.

Finally we remark that the singularities defined by Eq. (24), which we have not examined here, may be worth some additional study; however we note that in both the vacuum case,[30] $\xi = 0$, and in the case of planar Brillouin flow,[1,2,5,33] $\omega_p^2 = \omega_c^2$, the singularity, Eq. (24), is removable.

VII. Acknowledgments

We wish to thank I. Bernstein and P. Sprangle for several helpful discussions and A. M. Sessler for correspondence. Useful discussions with members of the Special Focus Program "Advanced Accelerators" are acknowledged.

This work was supported by the Office of Naval Research.

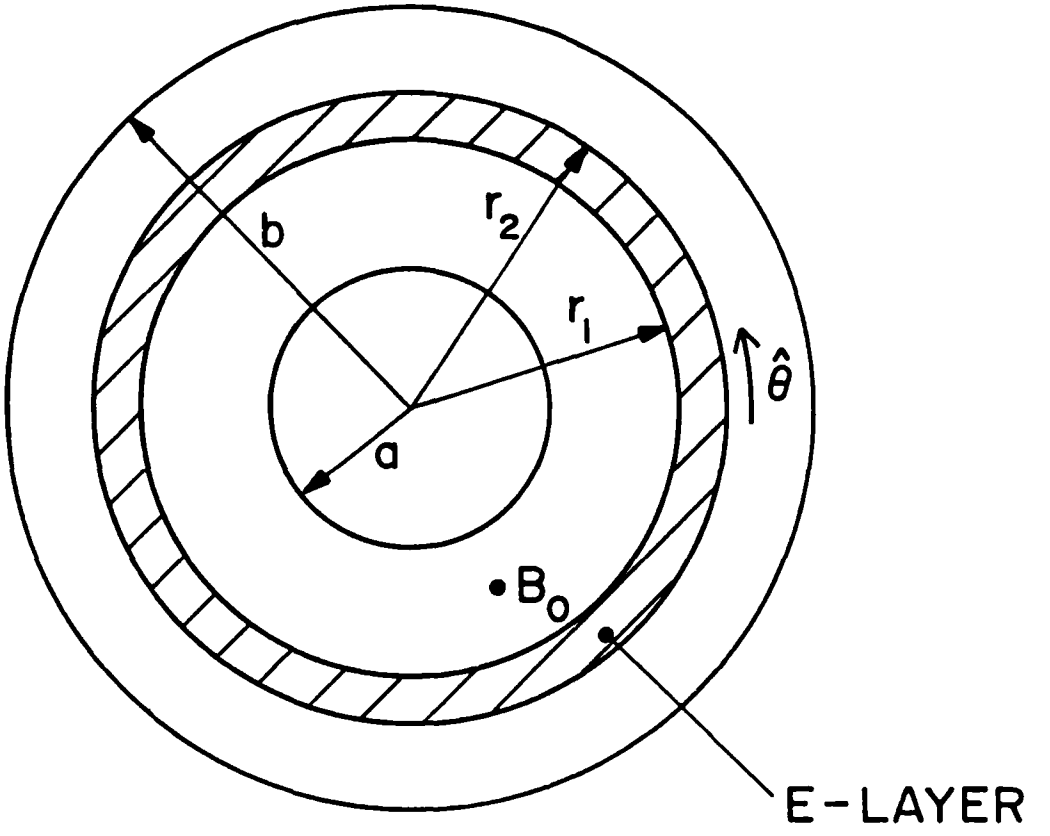

Fig. 1. Model of an E-layer. The layer, of infinite extent in z (in and out of the page), occupies the region $r_1 < r < r_2$ between the walls of a coaxial guide at r=a and r=b. The electrons, supported by an electric field $E_o(r)\hat{r}$ and a magnetic field $B_o(r)\hat{z}$, move in concentric circles in the equilibrium state, either clockwise or counterclockwise depending on the equilibrium type.

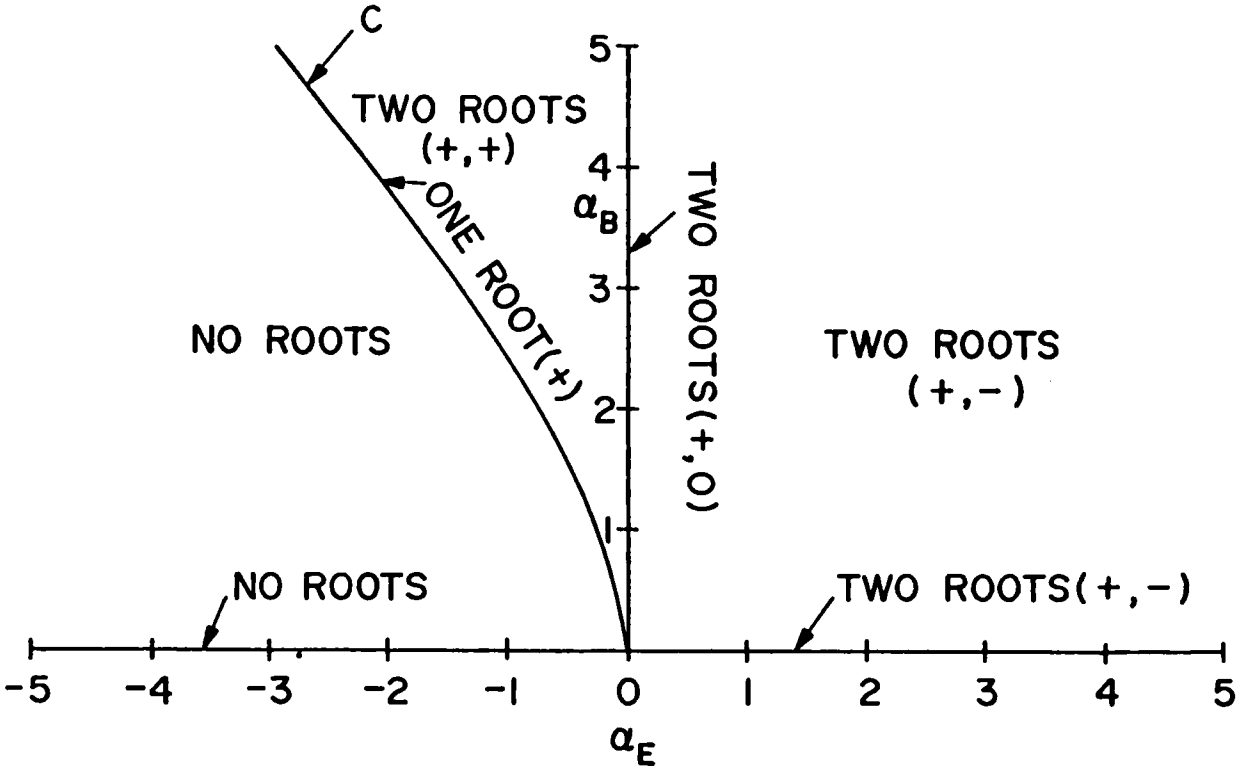

Fig. 2. The $\alpha_E - \alpha_B$ plane. The number and type of solutions to the equation of radial force balance (6) are shown in each region and on the boundaries between regions. A root is labeled + or - if it corresponds to clockwise or counterclockwise rotation respectively as one looks in the direction of $\hat{B}_o$.

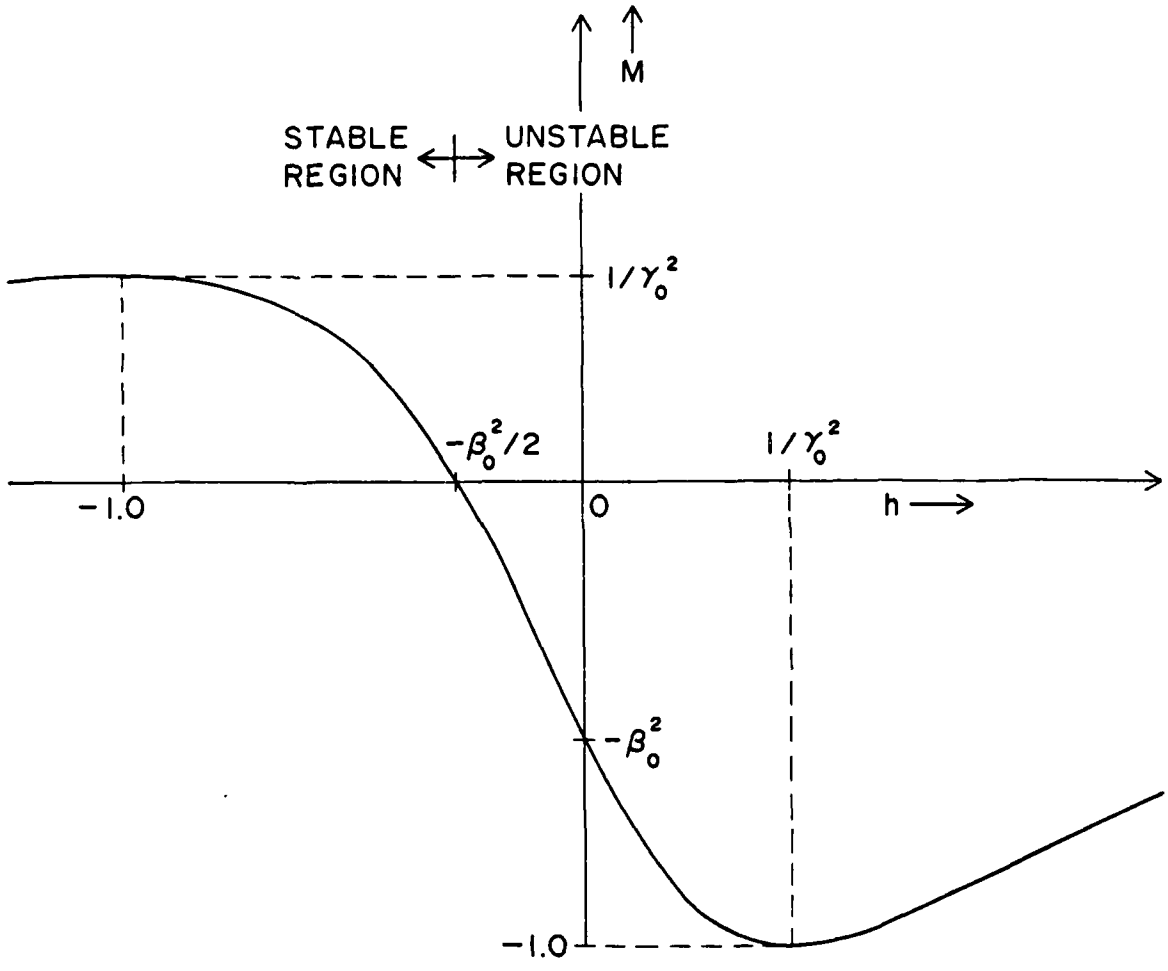

Fig. 3. Plot of the dimensionless "azimuthal mass" M versus the dimensionless equilibrium electric field, h. The actual plot shown is for the case $\gamma_0 = 1.5$ but all axis labels are expressed generally in terms of γ_0 or β_0.

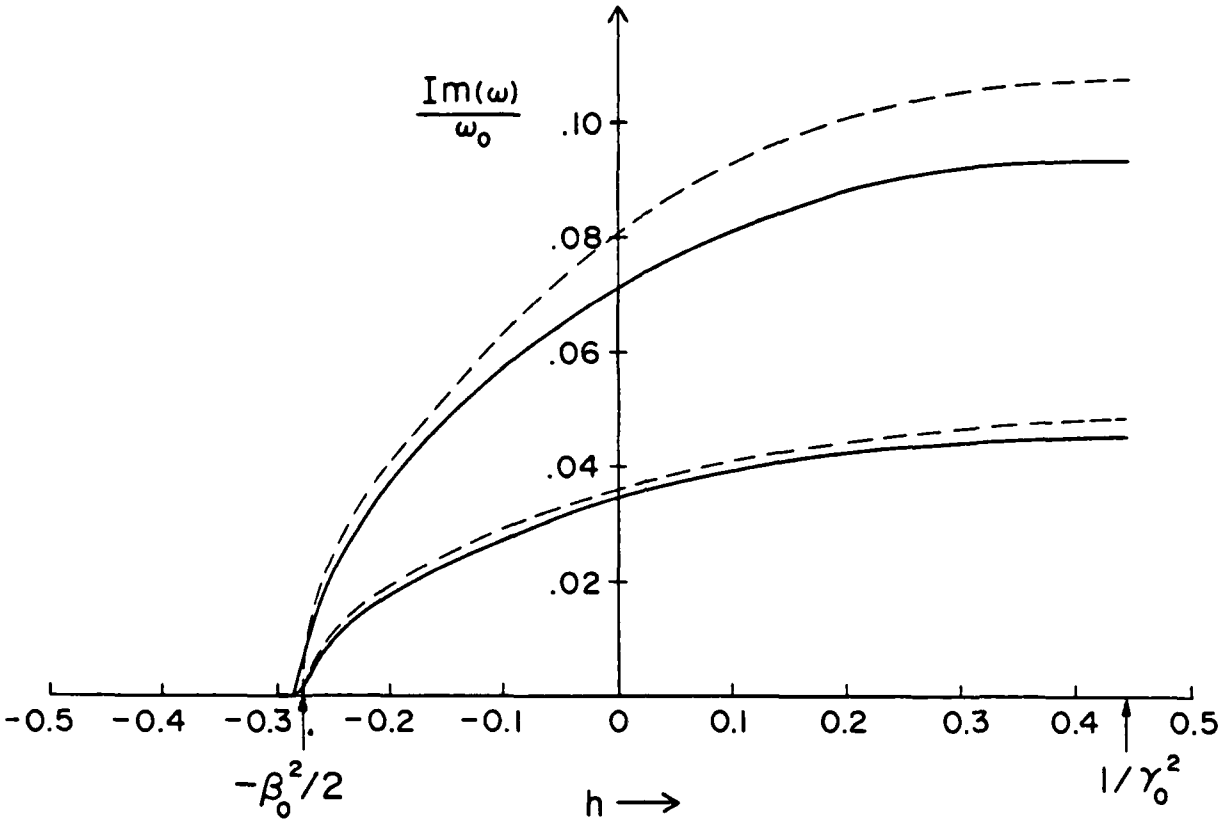

Fig. 4. Normalized growth rate for the negative mass instability versus h for the case a = 0.6m, b = 2.6m, R = 1.0m, $\tau/R = 0.02$, $\gamma_0 = 1.5$, $\ell = 1$. A solid curve indicates data obtained from a numerical solution of Eq. (14); the dashed line is a plot of Eq. (31). The upper pair of curves is for $\nu/\gamma_0 = 7.88 \times 10^{-3}$, $\xi = 1.42$; the lower pair is for $\nu/\gamma_0 = 1.57 \times 10^{-3}$, $\xi = 0.28$.

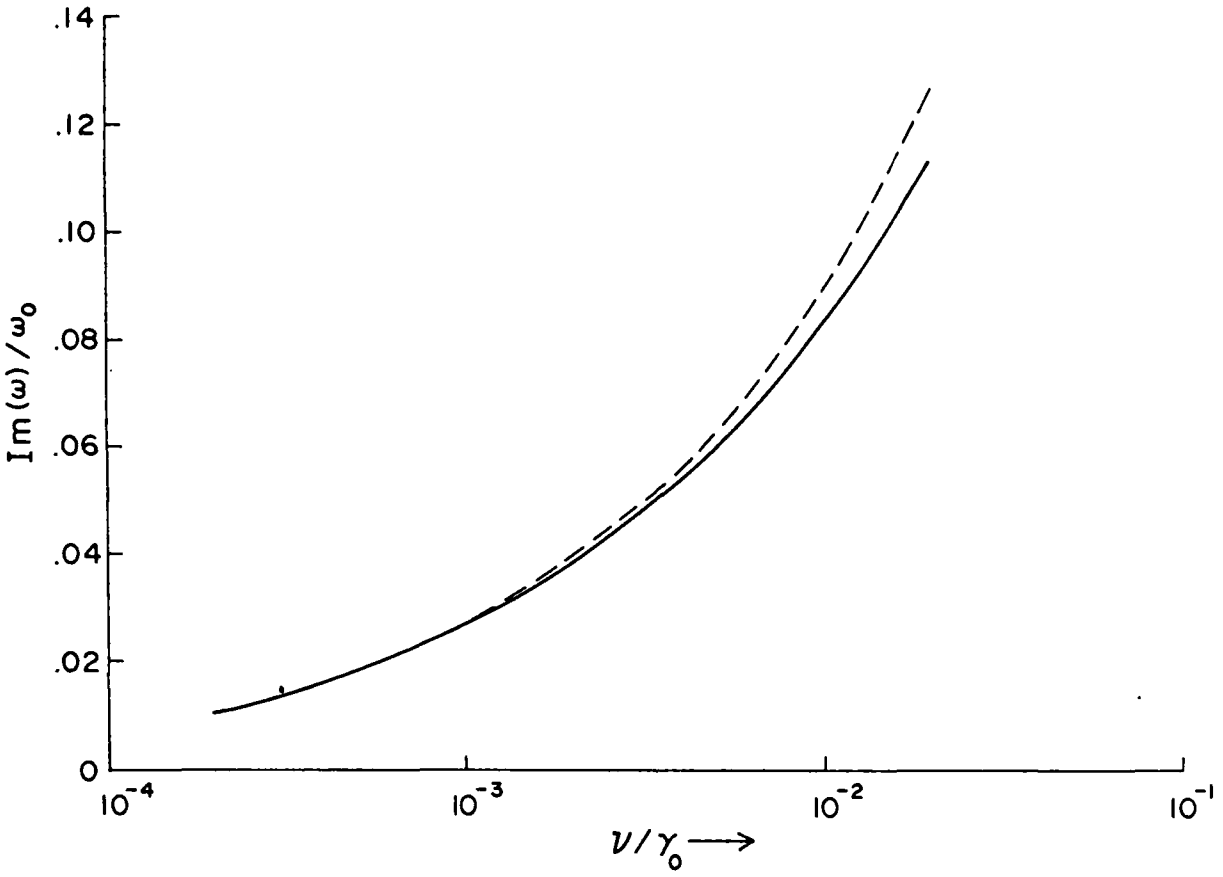

Fig. 5. Normalized growth rate for the negative mass instability versus ν/γ_o for the "base case" parameters: a = 0.5m, b = 2.2m, r_1 = 0.99m, r_2 = 1.01m, γ_o = 3, ℓ = 1. A solid curve denotes data obtained from a numerical solution of the eigenvalue problem; a dashed curve denotes data from the dispersion relation, Eq. (31).

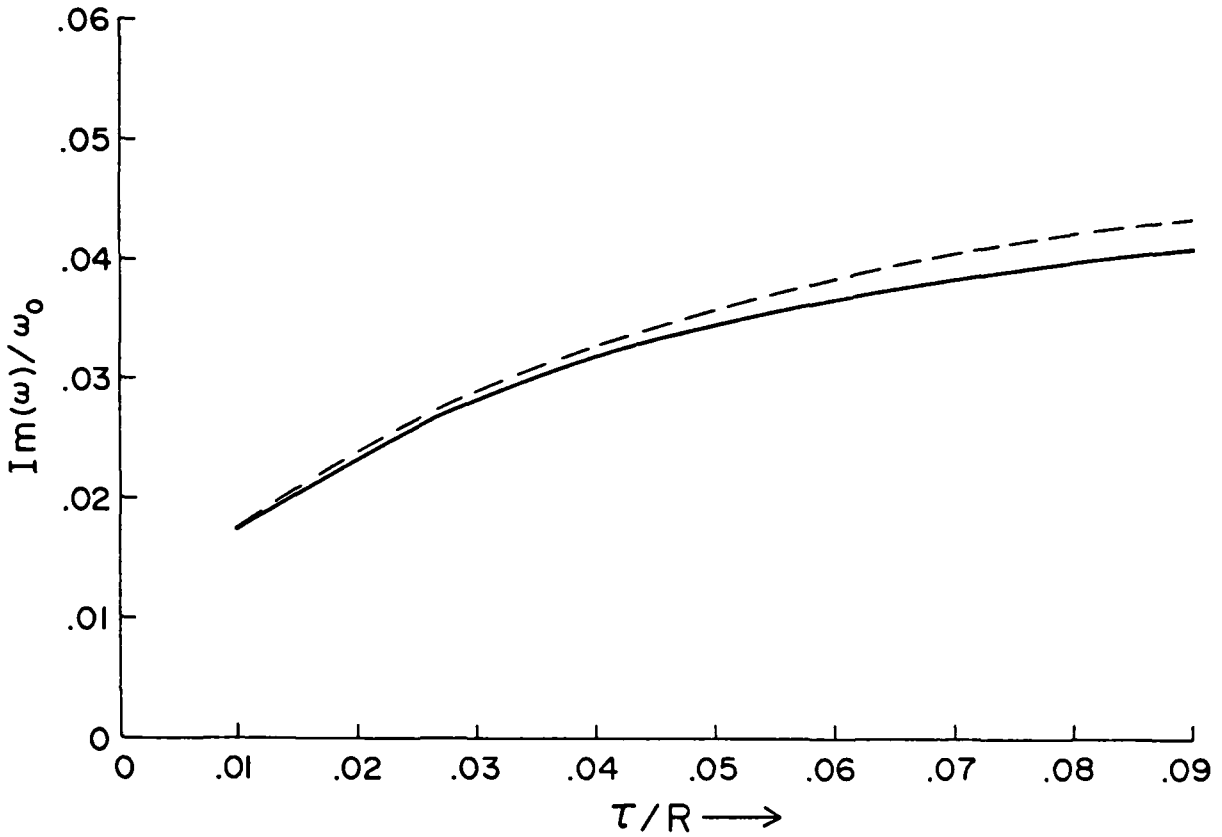

Fig. 6. Normalized growth rate for the negative mass instability versus layer thickness. All parameters take their base case values, (see text) except that the peak density in the parabolic profile is 10^7/cc.

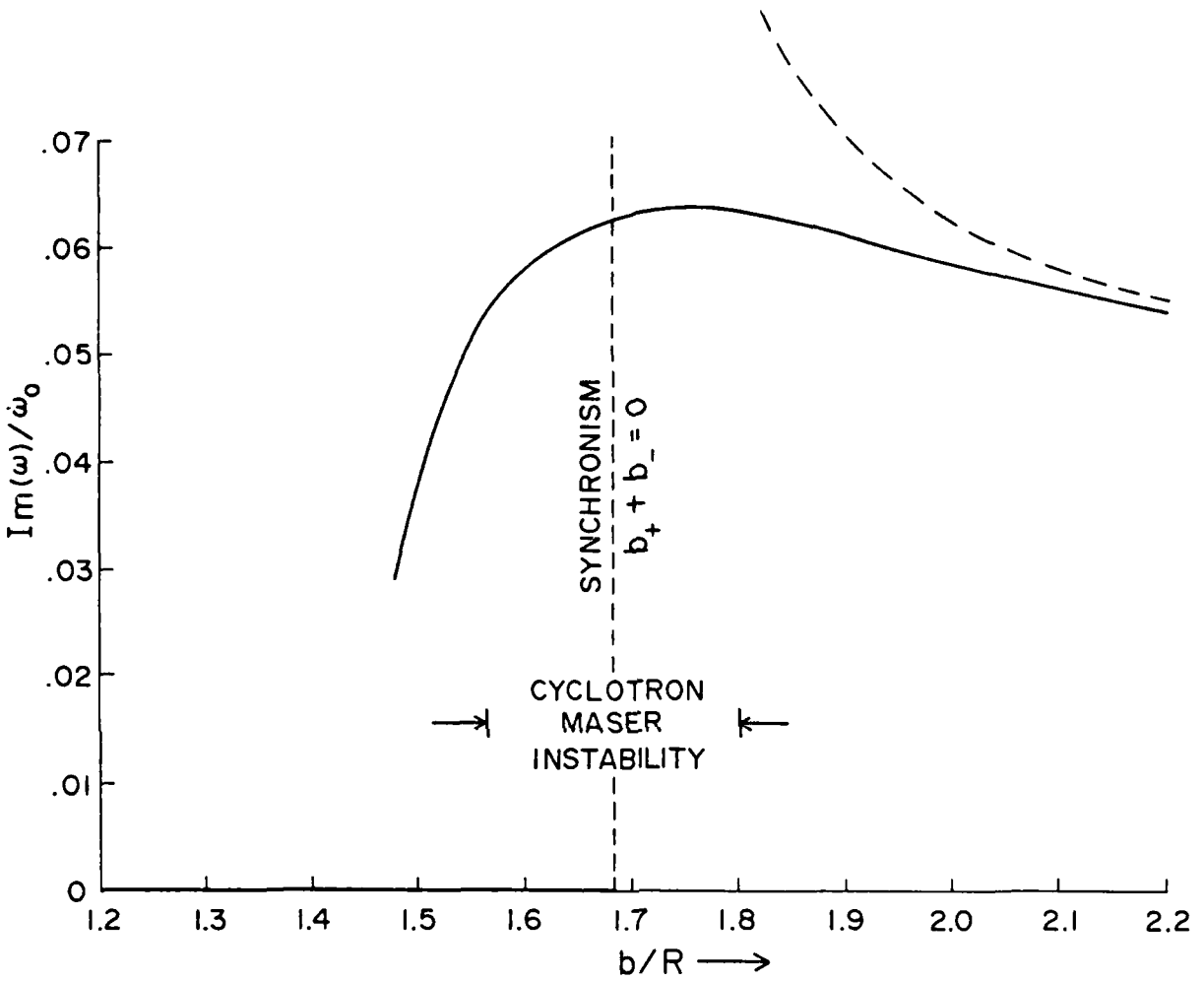

Fig. 7. Normalized growth rate for the negative mass instability versus outer wall position. All parameters take their base case values. (See text.) Near synchronous conditions, $\ell\omega_o \approx \omega_v$ where ω_v is a waveguide mode satisfying $b_+ + b_- = 0$, the negative mass instability is strongly enhanced and Eq. (31) should be solved as a cubic polynomial. The synchronous or enhanced negative mass instability is often called the cyclotron maser instability.

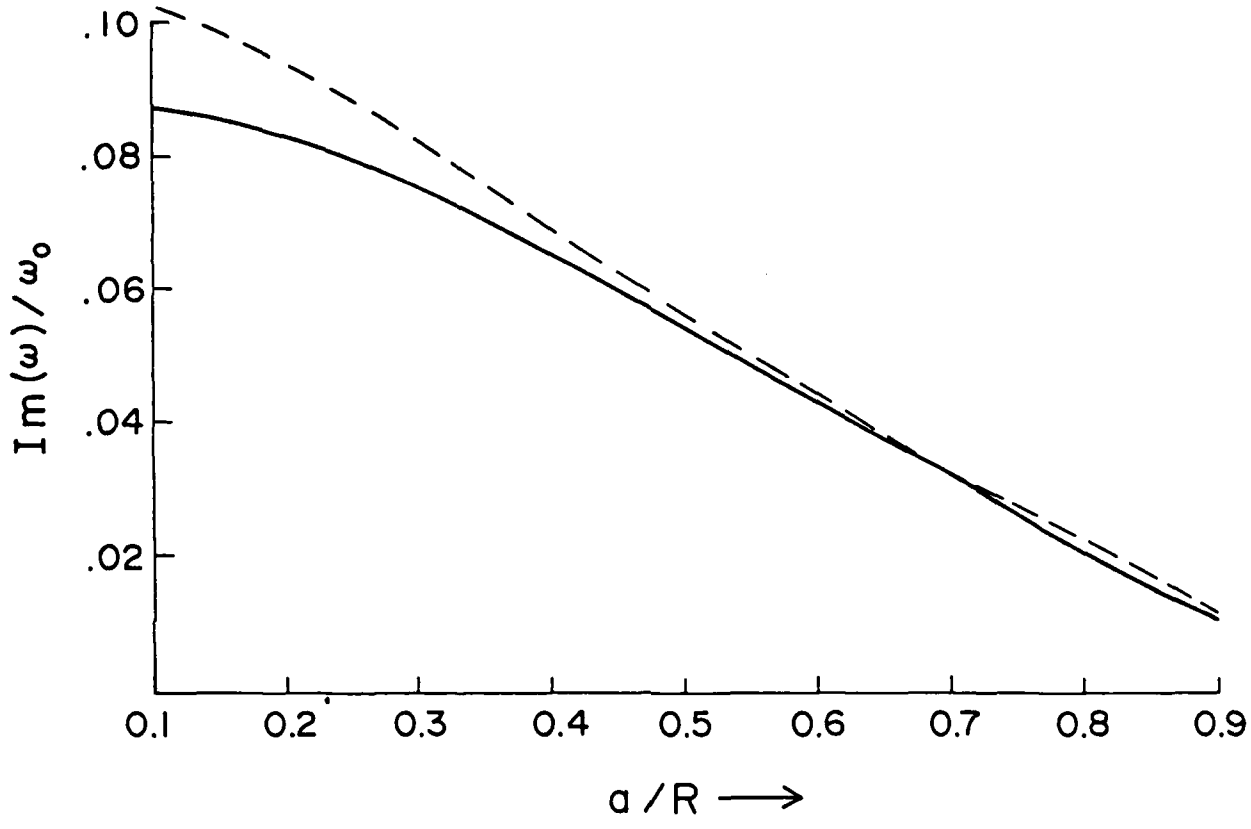

Fig. 8. Normalized growth rate for the negative mass instability versus inner wall position. All parameters take their base case values. (See text.)

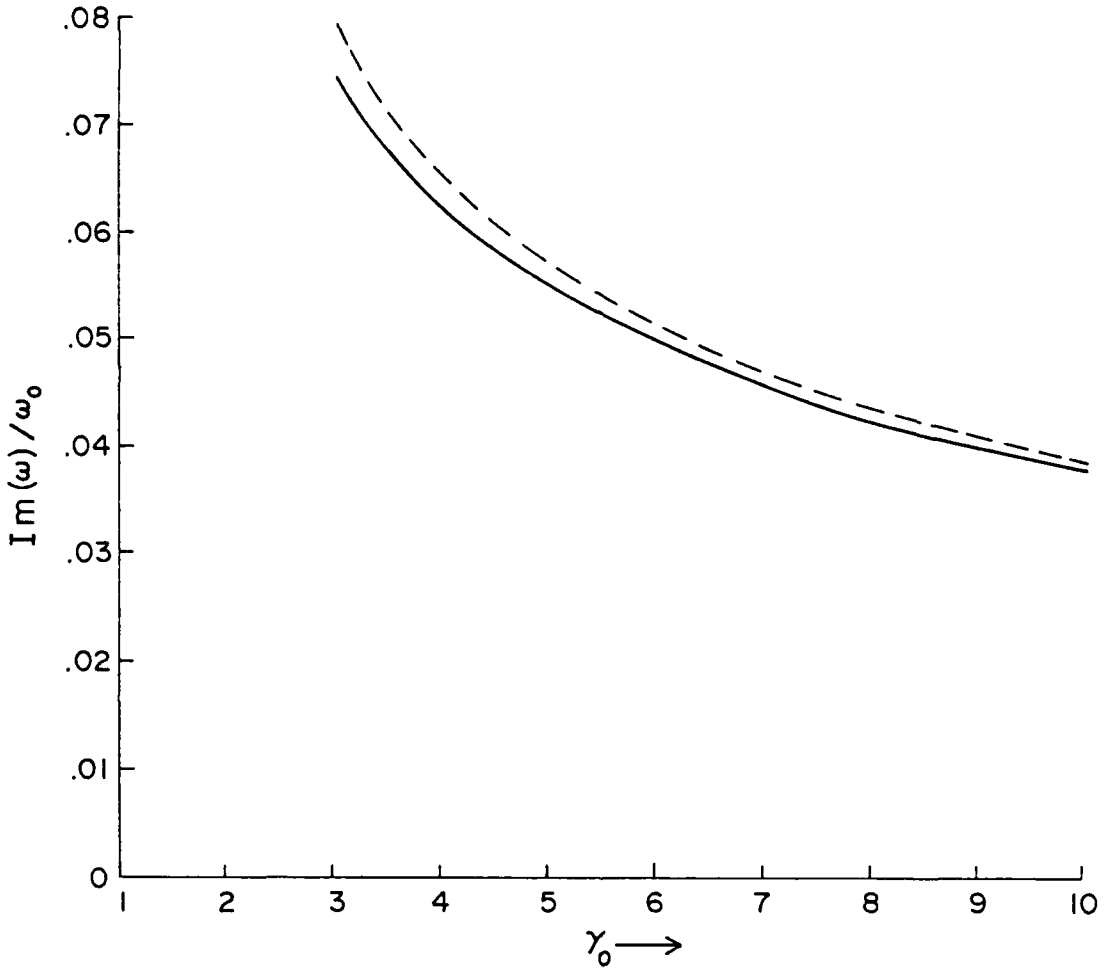

Fig. 9. Normalized growth rate for the negative mass instability versus γ_0. All parameters take their base case values, (see text) except that the peak density in the parabolic profile is 10^8/cc.

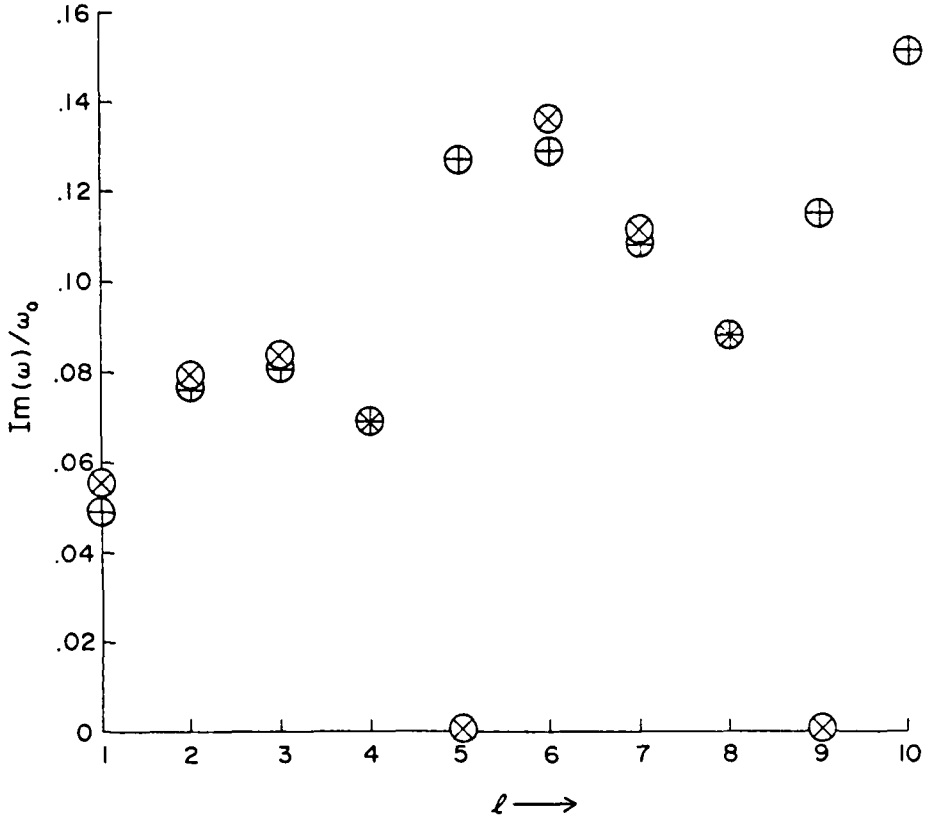

Fig. 10. Normalized growth rate for the negative mass instability versus azimuthal mode number ℓ. All parameters take their base case values. (See text.) A + denotes a result from Eq. (31) and an × denotes a result from a numerical solution of the eigenvalue problem.

Appendix A

Technique for Numerical Solution of Equilibrium Problem

In this Appendix we describe a simple technique based on Newton's method which we have used to solve a certain eigenvalue problem associated with the calculation of laminar E-layer equilibria. Given the electric field which is trivially solved for, having specified the density profile and potential on one wall, we must find the momentum profile, u(r) and the field $B_o(r)$ subject to the constraint of specified total flux Eq. (7). The total flux might be specified in an experiment in which a beam is injected and contained in a chamber for less than a magnetic diffusion time.

Let us cast the problem in terms of the dimensionless fields, α_E and α_B defined in the text following Eq. (6). The problem then is to find u(r) and $\alpha_B(r)$ subject to

$$\int_a^b dr\ \alpha_B \equiv F \equiv \text{specified constant} \qquad \text{(A-1)}$$

where u and α_B satisfy

$$u' = \frac{u}{r}\left[\frac{1-\xi/\gamma_o^2 - \gamma_o^2 h}{1+h}\right] \qquad \text{(A-2)}$$

$$\left(\frac{1}{r}\alpha_B\right)' = \frac{\omega_p^2}{c^2}u \qquad \text{(A-3)}$$

$$u^2 = \alpha_E(u^2+1)^{1/2} + \alpha_B u \qquad \text{(A-4)}$$

for $r_1 < r < r_2$. Equation (A-2) guarantees that if $u(r_1)$ satisfies Eq. (A-4) then u(r) will do so for all r. The algorithm proceeds as follows: An initial guess is made for $\alpha_B(r_1)$ using the value of the externally applied B field,

say. Using the known value of $\alpha_E(r_1)$ the roots (two, in general) of Eq. (A-4) are found and the one corresponding to the equilibrium of interest is chosen. Equations (A-2) and (A-3) are then integrated and the difference

$$\int_a^b dr\ \alpha_B - F \equiv D^* \qquad \text{(A-5)}$$

is calculated. $\alpha_B(r_1)$ is then adjusted according to

$$\alpha_{B,n+1} = \alpha_{B,n} - \frac{D^*}{\int_a^b dr \frac{\partial \alpha_{B,n}(r)}{\partial \alpha_{B,n}(r_1)}} \qquad \text{(A-6)}$$

where the subscript n denotes an iteration number. The loop is stopped once D* is less than some specified tolerance.

It remains only to describe the evaluation of the denominator in Eq. (A-6): The dependence of $\alpha_B(r)$ on its initial condition at r_1 is found during the integration of Eqs. (A-2) and (A-3) by simultaneously integrating the equations for $\partial\alpha_B(r)/\partial\alpha_B(r_1)$ and $\partial u(r)/\partial\alpha_B(r_1)$ which are simply obtained by explicitly differentiating Eqs. (A-2) and (A-3) with respect to $\alpha_B(r_1)$. The initial condition $\partial u(r_1)/\partial\alpha_B(r_1)$ is obtained from Eq. (A-4).

Appendix B

Evaluation of the TE Wave Admittances

In this Appendix the normalized admittances $b_\pm$ referred to in the text in Eqs. (21a,b) are given for the geometry of Fig. 1; the toroidal and planar cases are also discussed.

In the vacuum regions $a<r<r_1$ and $r_2<r<b$ the wave equation Eq. (14) is

$$r\frac{d}{dr}\left(\frac{r}{\frac{\omega^2 r^2}{c^2}-\ell^2}\frac{d\phi}{dr}\right)+\phi=0 \qquad \text{(B-1)}$$

the general solution to which is

$$\phi = x\left[C_1 J_\ell'(x) + C_2 Y_\ell'(x)\right] \qquad \text{(B-2)}$$

where $x = \omega r/c$, J_ℓ and Y_ℓ are the standard Bessel functions, C_1 and C_2 are constants, and in this Appendix a prime will denote $\frac{d}{dx}$. Note that the "singularities" at $x^2 = \ell^2$ in Eq. (B-1) are only apparent, not real, i.e. ϕ is analytic at these points. The other vacuum fields are

$$E_{1r} = \frac{i\ell}{x^2-\ell^2}\frac{d\phi}{dr}, \qquad \text{(B-3)}$$

$$B_{1z} = -\frac{x}{c\ell}E_{1r}. \qquad \text{(B-4)}$$

Using the definitions in the text Eqs. (21a,b), it follows that $b_\pm$ may be generally written

$$b_+ = -\frac{\ell}{x_2}\left[\frac{C_1^+ J_\ell(x_2) + C_2^+ Y_\ell(x_2)}{C_1^+ J_\ell'(x_2) + C_2^+ Y_\ell'(x_2)}\right] \qquad \text{(B-5a)}$$

$$b_- = \frac{\ell}{x_1}\left[\frac{C_1^- J_\ell(x_1) + C_2^- Y_\ell(x_1)}{C_1^- J'_\ell(x_1) + C_2^- Y'_\ell(x_1)}\right] \qquad \text{(B-5b)}$$

where $x_{1,2} \equiv \omega r_{1,2}/c$.

The ratios C_1^+/C_2^+ and C_1^-/C_2^- are determined by the boundary conditions at r=b and r=a respectively. Some special cases of interest are:

1. Perfectly conducting wall at $r=r_w$: (r_w= a or b)

$$C_1/C_2 = -Y'_\ell(x_w)/J'_\ell(x_w) \qquad \text{(B-6)}$$

2. Wall with (complex) dielectric $\varepsilon(\omega)$:

$$C_1/C_2 = -\left[\frac{Y'_\ell(x_w) - (\zeta/\zeta_o)Y_\ell(x_w)\frac{d}{dy}\ln Z(y)}{J'_\ell(x_w) - (\zeta/\zeta_o)J_\ell(x_w)\frac{d}{dy}\ln Z(y)}\right] \qquad \text{(B-7)}$$

where ζ is the surface impedance, $(\mu/\varepsilon)^{1/2}$, $\zeta_o = 376.7\Omega$, $y = \kappa r_w$, $\kappa = \omega(\varepsilon\mu)^{1/2}$, $Z(y) = J_\ell(y)$ for inner wall, $H_\ell^{(1)}(y)$ for outer wall where $H_\ell^{(1)}$ is the Hankel function. ε and μ refer to the wall material.

3. No inner wall:

$$C_2^- = 0 \qquad \text{(B-8)}$$

4. No outer wall:

$$C_1^+/C_2^+ = -i \qquad \text{(B-9)}$$

5. Electrostatic limit; perfectly conducting walls at r=a,b:

$$b_+ = \frac{B_+ + 1}{B_+ - 1} ; \qquad b_- = \frac{B_- + 1}{B_- - 1} \tag{B-10}$$

where $B_+ \equiv (b/r_2)^{2\ell}$ and $B_- \equiv (r_1/a)^{2\ell}$. Note that $b_\pm > 0$.

6. Planar limit ($r\to\infty$, $\ell\to\infty$; $\ell/r \equiv k_y$, $b-a$, $b-r_1$, $b-r_2$, r_2-r_1, all remain finite); perfectly conducting walls:

$$b_+ = - (k_y/\alpha) \cot [\alpha(r_1-a)] \tag{B-11}$$

$$b_- = - (k_y/\alpha) \cot [\alpha(b-r_2)] \tag{B-12}$$

where $\alpha \equiv (\omega^2/c^2 - k_y^2)^{1/2}$. The planar limit of (B-10) is just the electrostatic limit of (B-11) and (B-12), as expected, in which case

$$b_+ = \coth [k_y(b-r_2)] \tag{B-13}$$

$$b_- = \coth [k_y(r_1-a)]. \tag{B-14}$$

When a wall is resistive the resulting dissipation is represented by an imaginary part in the corresponding admittance $b_\pm$. (In Eq. (B-7) $\varepsilon(\omega) = i\sigma/\omega$ for a good conductor of conductivity σ.) That such dissipation can lead to disruptive beam instabilities, even for a "positive mass" beam, has been known since the pioneering work of Neil and Sessler[35] and Laslett, Neil, and Sessler.[36] It is in fact these resistive modes, rather than the (fundamentally dynamical) negative mass instability which are thought ultimately to limit the beam current in cyclic electron accelerators.

If a wall is not smooth but contains some structures (cavities, fins, etc.) a common practice is to calculate an approximate value for the admittance and to use it as a boundary condition for some approximation to Eq. (14) in the text. In this case however the problem is not being treated fully self consistently since the equilibrium of Section II would not be strictly correct, i.e., the correct equilibrium would no longer have azimuthal symmetry (and would be much harder to calculate).

For the case of a perfectly conducting wall we have plotted in Figs. B-1,2,3,4 the quantity $b_+ + b_-$ evaluated for $x_1 \cong x_2 \cong \ell\beta_o$ for various values of $E_\perp \equiv mc^2(\gamma_o - 1)$, assuming a thin layer. It is this quantity, $b_+ + b_-$, which enters the dispersion relation for the longitudinal mode discussed in the text.

For a toroidal (accelerator) geometry, the dispersion relation Eq. (31) is expected to be replaced by

$$\Omega_1^2 = -\varepsilon_o g \ell^2 (2\nu/\gamma_o)(c^2/R^2)(mc^2/\omega_o)(\partial\omega_o/\partial\varepsilon)_{ext} \qquad \text{(B-15)}$$

where $(\partial\omega_o/\partial\varepsilon)_{ext}$ denotes the derivative of the circulation frequency with respect to total particle energy evaluated as if the particle were acted upon only by the external electric and magnetic fields. In Eq. (B-15), we have identified the geometric factor g of refs. [8,11] with $1/\left(\ell\varepsilon_o(b_+ + b_-)\right)$, as pointed out in ref. 10. Note that the dispersion relationship (B-15) includes self field effects and that g is always positive for toroidal geometry (with smooth, perfectly conducting walls).

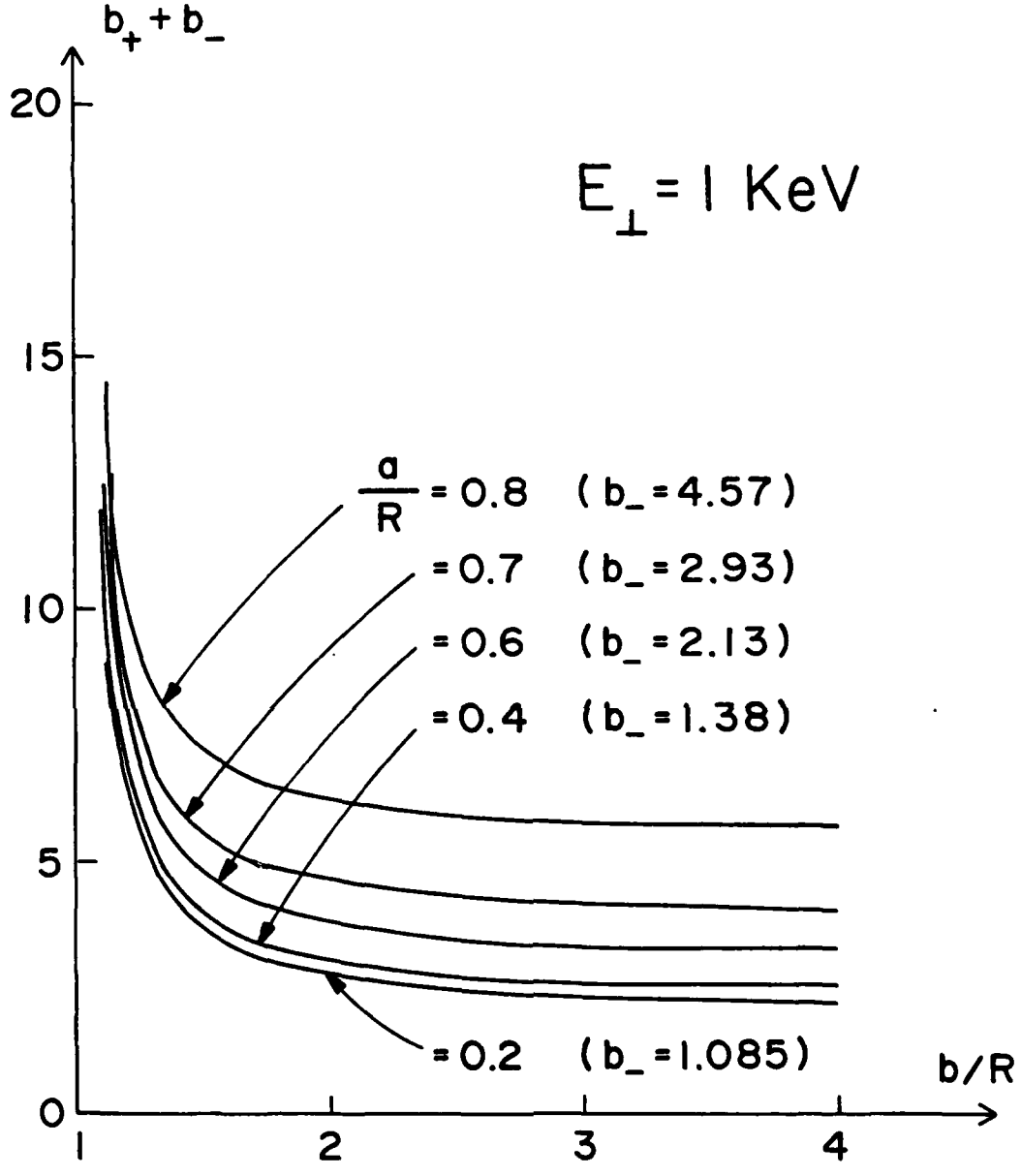

Fig. B-1. Normalized admittances vs. outer wall position for various inner wall positions for $\ell = 1$ and $mc^2(\gamma_o - 1) = 1$ keV.

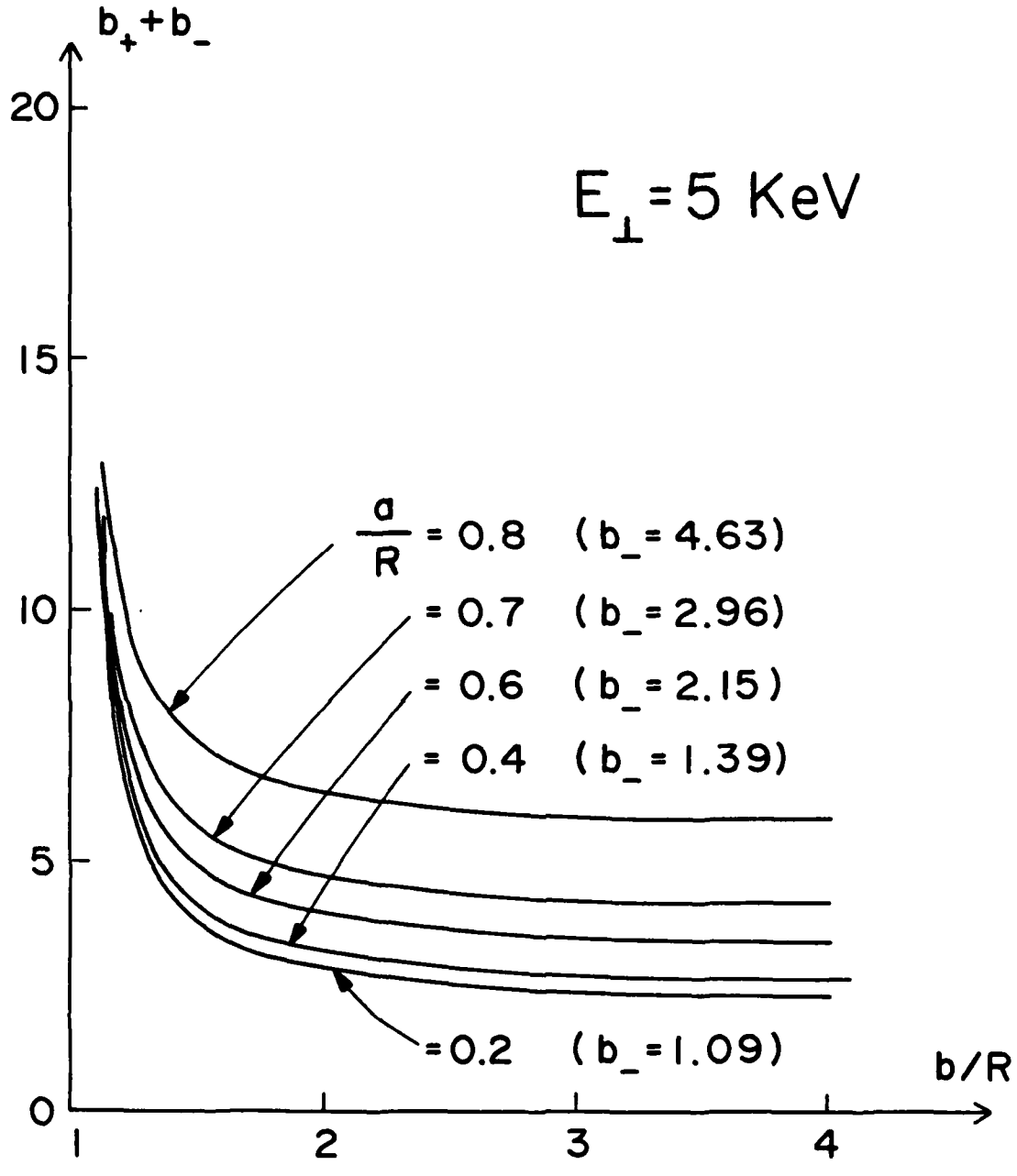

Fig. B-2. As in Fig. B-1 but for $mc^2(\gamma_o - 1) = 5$ keV.

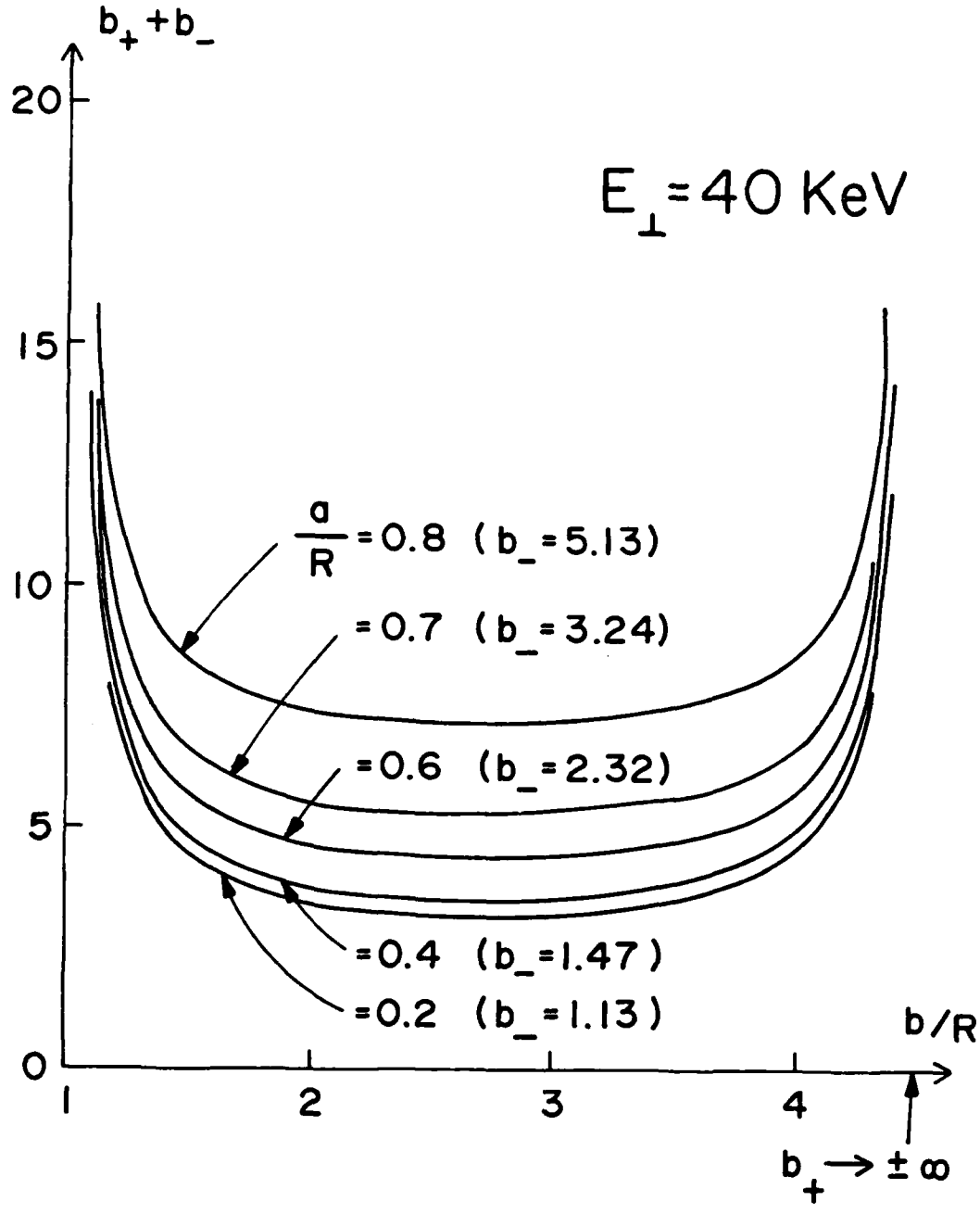

Fig. B-3. As in Fig. B-1 but for $mc^2(\gamma_o - 1) = 40$ keV.

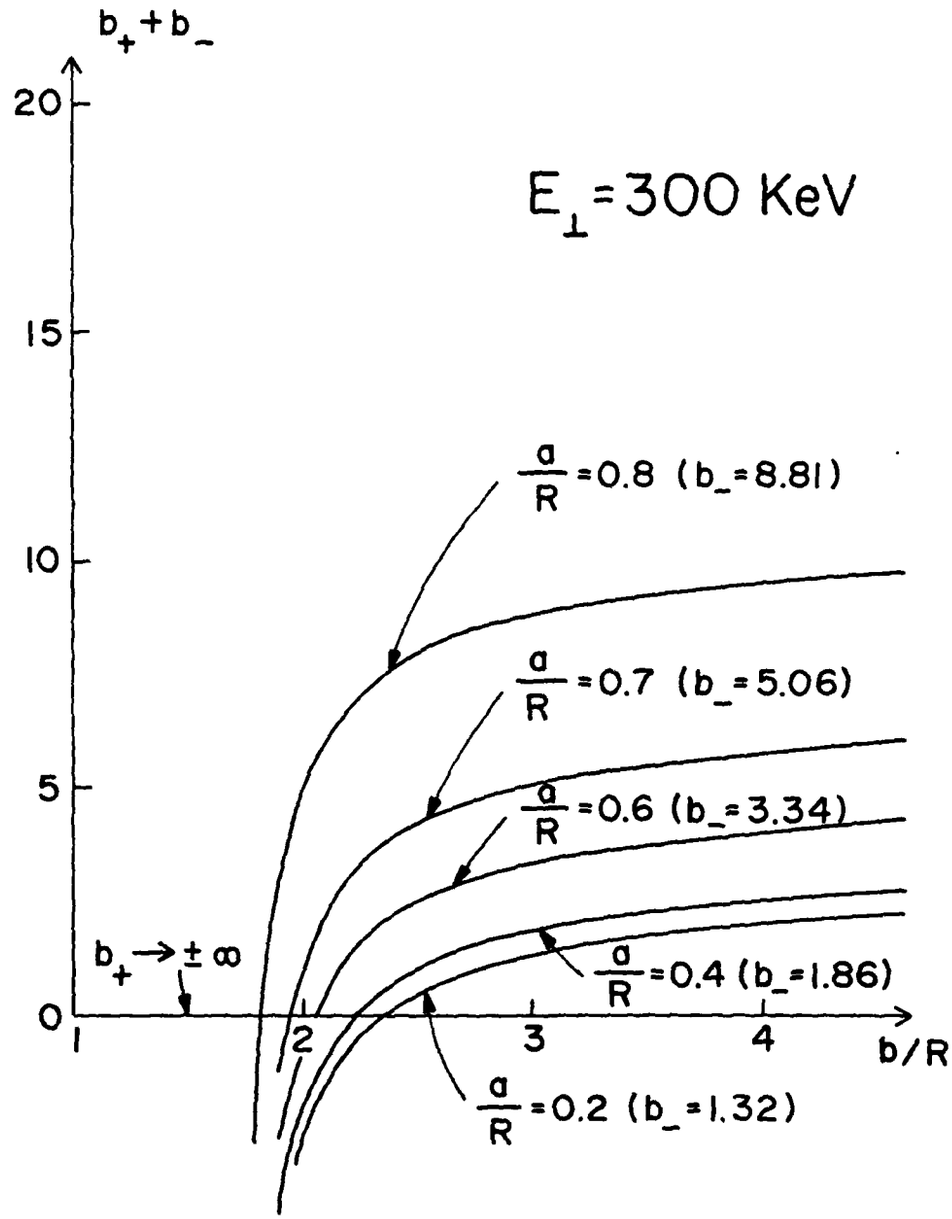

Fig. B-4. As in Fig. B-1 but for $mc^2(\gamma_o - 1)$ = 300 keV. The zeroes of $b_+ + b_-$ correspond to waveguide cutoff frequencies.

References

1. G. C. MacFarlane and H. G. Hay, Proc. Phys. Soc. (London) B63, 409 (1950).
2. O. Buneman, in Proc. Conf. Dynamics of Ionized Media, R.L.F. Boyd, ed. (University College, London, 1951).
3. J. R. Pierce, IRE Trans. Electron Devices ED-3, 183 (1956).
4. O. Buneman, J. Electron. Control 3, 1,507 (1957).
5. O. Buneman, in Crossed-Field Microwave Devices, E. Okress, ed. (Academic Press, New York, 1961), Vol. 1, pp. 209ff and 367ff.
6. R. H. Levy, Phys. Fluids 8, 1288 (1965).
7. O. Buneman, R. H. Levy and L. M. Linson, J. Appl. Phys. 37, 3203 (1966).
8. C. E. Nielsen, A. M. Sessler and K. R. Symon, in Proc, Intl. Conf. on High-Energy Accelerators and Instrumentation (Geneva), p. 239, (1959).
9. A. A. Kolomenskii and A. N. Lebedev, ibid., p. 115.
10. R. J. Briggs and V. K. Neil, J. Nucl. Energy C9, 209 (1967).
11. R. W. Landau and V. K. Neil, Phys. Fluids 9, 2412 (1966).
12. J. D. Callen and C. W. Horton, Phys. Fluids 13, 154 (1970).
13. R. W. Landau, Phys. Fluids 11, 205 (1968).
14. R. Q. Twiss, Aust. J. Phys. 11, 564 (1958).
15. J. Schneider, Phys. Rev. Lett. 2, 504 (1959).
16. A. V. Gaponov, Izu. VUZ., Radiofizika 2, 450 (1959) and addendum, ibid., p. 836.
17. Some suggested review articles are:

    J. L. Hirshfield and V. L. Granatstein, IEEE Trans. Microwave Theory Tech. MTT-25, 522 (1977).

    V. A. Flyagin, A. V. Gaponov, M. I. Petelin and V. K. Yulpatov, ibid., p. 514.

    P. Sprangle and A. T. Drobot, ibid., p. 528.

A. A. Andronov, et. al., Infrared Phys. 18, 385 (1978).

J. L. Hirshfield in Infrared and Millimeter Waves Vol. I, K. J. Button, ed. (Academic Press, New York, 1979) pp. 1-54.

R. S. Symons and H. R. Jory in Advances in Electronics and Electron Physics Vol. 55, C. Marton, ed. (Academic Press, New York, 1981).

V. L. Granatstein, M. Read and L. R. Barnett., Inter. J. Infrared and Millimeter Waves, 5 (1982).

Y. Y. Lau, IEEE Trans. Electron Devices 29, 320 (1982).

18. Y. Y. Lau, IEEE Trans. Electron Devices 31, 329 (1984).
19. N. Rostoker, Part. Accel. 5, 93 (1973).
20. C. A. Kapetanakos, P. Sprangle, D. P. Chernin, S. J. Marsh and I. Haber, Phys. Fluids 26, 1634 (1983).
21. J. M. Finn and W. M. Manheimer, Phys. Fluids 26, 3400 (1983).
22. P. Sprangle and D. Chernin, Part. Accel. (in press).
23. N. C. Christofilos in Proc. of the Second Intl. Conf. on the Peaceful Uses of Atomic Energy (Geneva) Vol. 32, p. 279, (1958).
24. I. Alexeff and F. Dyer, Phys. Rev. Lett. 43, 351 (1980). See also, L. R. Barnett, doctoral dissertation, Univ. of Tennessee, Knoxville (1978), for a related device.
25. G. Dohler, submitted to IEEE Trans. Electron Devices (1983).
26. R. H. Pantell, IRE Trans. Electron Devices ED-7, 22 (1960).
27. Some analytical and numerical work, with different applications in mind, has been reported by B. Godfrey, IEEE Trans. Plasma Sci. PS-7, (1979).
28. Y. Y. Lau and D. Chernin, Phys. Rev. Lett. 52, 1425 (1984).
29. R. C. Davidson and K. Tsang, Bull. Am. Phys. Soc. 28, 1211 (1983).
30. Y. Y. Lau and R. J. Briggs, Phys. Fluids 14, 967 (1971).

31. It is also possible, of course, to expand the eigenfunction ϕ about any of the singularities of Eq. (14). If this is done for the longitudinal mode an expression similar to Eq. (26) but containing certain logarithmic terms is obtained; these log terms may be shown to be stabilizing. Such an expansion about $\Omega = 0$ was used to obtain the second order term given in Eq. (36). Of course if both series, about $r = R$ and about $\Omega = 0$, are convergent then they must give identical results for the dispersion relation. We should point out that the transverse modes may also be studied via an expansion about the mid point $r = (r_1 + r_2)/2$, whereas an expansion about $\Omega = 0$ focuses only on the longitudinal modes.

32. R. J. Briggs and V. K. Neil, J. Nucl. Energy C8, 255 (1966).

33. J. Swegle and E. Ott, Phys. Fluids 24, 1821 (1981); also, J. Swegle, Phys. Fluids 26, 1670 (1983).

34. D. Chernin, Phys. Fluids 25, 1342 (1982).

35. V. K. Neil and A. M. Sessler, Rev. Sci. Instr. 36, 429 (1965).

36. L. S. Laslett, V. K. Neil and A. M. Sessler, Rev. Sci. Instr. 36, 436 (1965).

37. C. L. Chang, T. M. Antonsen, Jr., E. Ott and A. T. Drobot, submitted to Phys. Fluids (1983).

38. V. K. Neil and W. Heckrotte, J. Appl. Phys. 36, 2761 (1965).

39. M. A. Mostrom and M. E. Jones, Phys. Fluids 26, 1649 (1983).

END

FILMED